

# Contemporaneous plutonism and strike-slip faulting: A case study from the Tonale fault zone north of the Adamello pluton (Italian Alps)

M. Stipp<sup>1</sup> and B. Fügenschuh

Department of Earth Sciences, Basel University, Basel, Switzerland

L. P. Gromet

Department of Geological Sciences, Brown University, Providence, Rhode Island, USA

H. Stünitz and S. M. Schmid

Department of Earth Sciences, Basel University, Basel, Switzerland

Received 25 February 2003; revised 10 November 2003; accepted 11 February 2004; published 15 May 2004.

[1] A field, microstructural, and geochronological study of contemporaneous plutonism and strike-slip faulting along the eastern Tonale fault zone provides new insights into the interrelationships between magmatic emplacement, contact metamorphism and shearing, and it places new time constraints for the Periadriatic Fault System. Although pluton emplacement and shearing were not caused by each other, they mutually interacted during contact metamorphism. The character of the composite Tonale fault zone varies considerably with its proximity to the northern margin of the Adamello pluton, from a paired greenschist facies mylonite belt (Northern mylonite zone) and cataclastic fault zone in the west, to a fault zone consisting of Northern mylonite zone, Cataclastic fault zone and a second mylonite belt (Southern mylonite zone) formed by contemporaneous shearing and contact metamorphism in the east. Ongoing strike-slip motion led to telescoping and advective cooling of the deforming contact aureole. New U/Pb zircon ages for the northernmost Adamello intrusions (the Avio at 34.6–1.0 Ma and the Presanella at 32.0–2.3 Ma) date the onset of contact metamorphism. Rb-Sr and K-Ar cooling ages and new zircon fission track ages provide evidence that postintrusive cooling to below 300°C was achieved rapidly, i.e., approximately 30 Myr ago being consistent with a shallow crustal emplacement at ambient temperatures of approximately 250°C. Cataclastic dextral strike-slip faulting continued until about 20 Ma, when the Tonale fault zone became offset by a number of minor sinistral shears, and by the

Giudicarie fault. Hence dextral strike-slip motion along the Periadriatic Fault System east of the Bergell pluton lasted from approximately 35–20 Myr ago. *INDEX TERMS*: 8010 Structural Geology: Fractures and faults; 8030 Structural Geology: Microstructures; 8035 Structural Geology: Pluton emplacement; 8110 Tectonophysics: Continental tectonics—general (0905); 9335 Information Related to Geographic Region: Europe; *KEYWORDS*: strike-slip faulting, intrusion, contact metamorphism, dating, recrystallization, Alpine orogeny. **Citation**: Stipp, M., B. Fügenschuh, L. P. Gromet, H. Stünitz, and S. M. Schmid (2004), Contemporaneous plutonism and strike-slip faulting: A case study from the Tonale fault zone north of the Adamello pluton (Italian Alps), *Tectonics*, 23, TC3004, doi:10.1029/2003TC001515.

## 1. Introduction

[2] Plutonism is commonly related to major crustal fault zones, and syntectonic intrusions have been described in several recent studies [e.g., Davidson *et al.*, 1992; Rosenberg *et al.*, 1995; Brown and Solar, 1999; Bodorkos *et al.*, 2000; Steenken *et al.*, 2000; Andronicos *et al.*, 2003; Moya *et al.*, 2003]. Eocene-Oligocene plutonism [e.g., Laubscher, 1983; von Blanckenburg *et al.*, 1998] is widespread along the Periadriatic Fault System (or Periadriatic Lineament), the largest and most important fault system in the Alps, extending over 700 km from west (Piemonte, NW Italy) to east (Karawanken, Austrian-Slovenian border) and separating the main body of the Alps (the Western, Central and Eastern Alps) from the Southern Alps. So far synkinematic intrusive emplacement has been demonstrated, e.g., for the Bergell [e.g., Rosenberg *et al.*, 1995; Berger *et al.*, 1996; Schmid *et al.*, 1996], the Rieserferner [e.g., Steenken *et al.*, 2000] and the Karawanken pluton [e.g., von Gosen, 1989]. On the basis of these studies, Rosenberg [2004] suggests that magma ascent and emplacement are synkinematic all along the Periadriatic Fault System.

[3] However, the exact relationships between the emplacement of the Adamello pluton and movements along the eastern part of the Tonale fault zone (part of the Periadriatic

<sup>1</sup>Now at Geological Institute, Albert-Ludwigs-University, Freiburg, Germany.

Fault System; Figure 1) have not yet been established and are hence subject of this study. Note, that the Adamello pluton occupies an exceptional position among the Periadriatic intrusions, being situated within the South-Alpine block, i.e., south (rather than north) of the Periadriatic Fault System. Furthermore, the Adamello is the largest of the Periadriatic plutons. It intruded over a considerably longer time span in comparison to all other Periadriatic intrusions: cooling and presumably emplacement of the different intrusive units progressively moved from south to north [e.g., *Del Moro et al.*, 1983], i.e., towards the Tonale fault zone. Regarding the southern intrusions, emplacement was primarily forceful by stoping, and partly by ballooning [*Brack*, 1983]. Ascent and emplacement in the north and at the contact to the adjacent Tonale fault zone, and hence the relationships with the possibly contemporaneous movements along the Periadriatic Fault System, are still ill constrained. Observations from this area appear contradictory at first sight: *Mendum* [1976] and *Werling* [1992] provided evidence for ballooning, *Werling* [1992] and *Stipp et al.* [2002a, 2002b] claim contact metamorphism and mylonitization within the Tonale fault zone to be synchronous, and finally, *Martin et al.* [1991] and *Stipp et al.* [2002a] describe solid state deformation overprint in the northernmost margin of the Adamello pluton. Hence a comprehensive study leading to a consistent model for the emplacement of the northern Adamello intrusions, including the temporal and spatial relationships to the movements along the Tonale fault zone, is still lacking.

[4] Another problem is that the different segments of the Periadriatic Fault System differ in terms of fault plane orientation, fault rock composition, as well as kinematics and timing of movements [e.g., *Cornelius and Furlani-Cornelius*, 1930; *Bögel*, 1975; *Ahrendt*, 1980; *Schmid et al.*, 1989]. Numerous field studies address timing and kinematics of the various fault segments [e.g., *Fumasoli*, 1974; *Lardelli*, 1981; *Vogler and Voll*, 1981; *Wiedenbeck*, 1986; *Heitzmann*, 1987; *Schmid et al.*, 1987; *Zarske*, 1989; *Martin et al.*, 1991; *Werling*, 1992; *Berger et al.*, 1996; *Prosser*, 1998; *Mancktelow et al.*, 2001; *Müller et al.*, 2001; *Viola et al.*, 2001]. In spite of these studies, age, amount and duration of dextral strike-slip movements along the EW striking fault segments are still unclear and highly debated. The close spatial relationships of the Adamello pluton to the dextrally active Tonale fault zone, and to the sinistrally active Giudicarie fault (Figure 1), potentially provide a chronological framework for answering these open questions that are important for understanding the relationships between pluton ascent and emplacement and transpressive and/or strike-slip movements along the most spectacular lineament of the European Alps: the Periadriatic Fault System.

[5] In summary, the scope of this study is multiple. We aim at (1) unraveling spatial and temporal relationships between plutonism and strike-slip faulting, (2) understanding mutual feedbacks between shearing and contact metamorphism that can be exceptionally well observed in the study area, (3) providing exact dating constraints regarding the age of intrusion, as well as cooling ages in the northern

Adamello pluton, not available up to now, but crucial for unraveling the timing of the various kinematic stages during a long history of movements along this 700 km long Periadriatic Fault System.

## 2. Regional Setting

[6] The western segment of the Tonale fault zone, situated west of our study area and adjacent to the Bergell intrusion, primarily represents a greenschist-facies mylonite belt. There, the mylonites separate the exhumed amphibolite facies part of the central Alps from the Southern Alps, which are unaffected by Alpine metamorphism. The E-W striking mylonites exhibit steep foliations, carrying stretching lineations changing from a down-dip orientation in the north, related to backthrusting, to a subhorizontal orientation in the south, related to dextral strike-slip [*Vogler and Voll*, 1981; *Heitzmann*, 1987; *Fisch*, 1989; *Schmid et al.*, 1989]. Metamorphic grade during mylonitization within the western Tonale fault zone systematically decreases from north to south, as is expected for a scenario of backthrusting which, in combination with erosion, exhumes the amphibolite-grade central Alps. Backthrusting and dextral strike-slip occurred in an overall transpressive tectonic scenario [*Schmid et al.*, 1989]. However, at their southern rim these mylonites are overprinted by a vertical E-W striking dextral cataclastic fault zone [*Fumasoli*, 1974]. This cataclastic fault zone, together with the southernmost and colder part of the mylonite belt, exclusively records strike-slip movements.

[7] East of the Bergell intrusion, i.e., towards the area of this study, the amount of backthrusting diminishes over a relatively short distance [*Schmid et al.*, 1989]. Only subhorizontal stretching lineations have been observed within the Tonale fault zone east of the Bergell intrusion [*Wiedenbeck*, 1986; *Werling*, 1992]. This work focuses on the easternmost part of the Tonale fault zone, also characterized by predominant dextral strike-slip motion, observed all the way from Monte Padrio (northwest of Edolo) to Dimaro in the east, where the Tonale fault zone appears to be offset by the Giudicarie line (Figure 1). This easternmost Tonale fault zone is close to or at the northern margin of the Adamello pluton (Figure 2), and it separates a southernmost Austro-Alpine unit (Tonale unit) in the North from the basement of the Southern Alps and/or the Adamello pluton in the South.

[8] The Tonale unit consists of amphibolite facies metamorphic rocks of Variscan age [e.g., *Salomon*, 1905; *Hammer and Trener*, 1908; *Andreatta*, 1935; *Mendum*, 1976]. Alpine greenschist-facies metamorphic overprint is weak and only observed in mylonitic shear zones, such as the Stavel mylonites (Figure 2) [*Werling*, 1992], or older Alpine shear zones situated north of the Tonale fault zone [*Martin et al.*, 1991; *Müller*, 1998; *Viola*, 2000].

[9] The basement of the Southern Alps consists of the so-called “Edolo schists,” a monotonous series of dark gray graphitic phyllites with varying quartz content and intercalated quartzites [*Cornelius and Furlani-Cornelius*, 1930; *Gansser*, 1968]. The Edolo schists are characterized

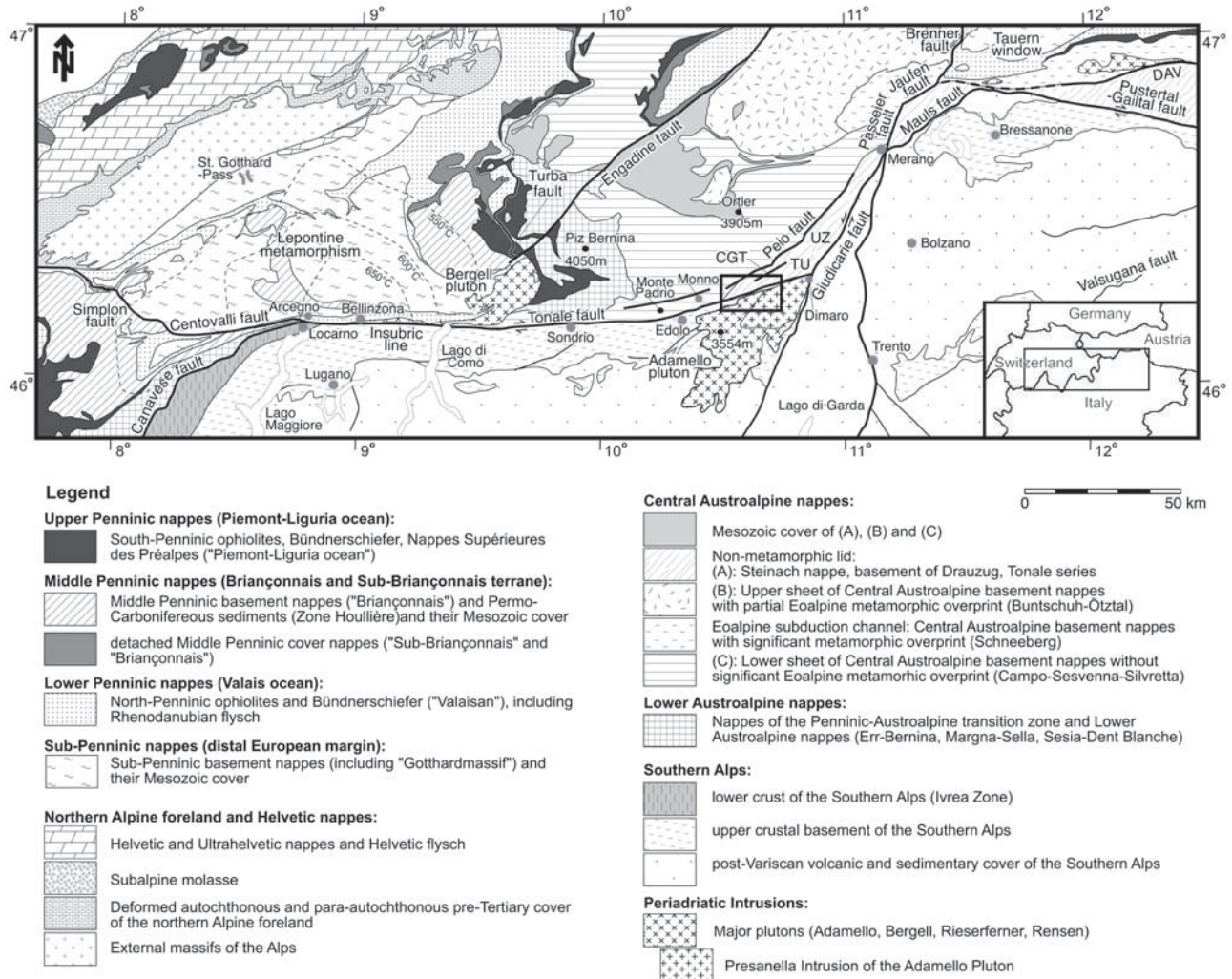


**Figure 1.** Regional (tectonic and geographical) position of area of study (rectangular frame, location of Figure 2); abbreviations are as follows: CGT, Cima Grande thrust; DAV, Defereggen-Antholz-Vals (fault); TU, Tonale unit; UZ, Ulten zone. Isotherms related to Lepontine metamorphism are from *Frey et al.* [1999].

by pre-Alpine polyphase deformation under amphibolite and retrograde greenschist facies conditions [Spalla *et al.*, 1999]. In the Tertiary, the Edolo schists were affected by contact metamorphism associated with the emplacement of the composite Adamello pluton [Trenner, 1906; Mendum, 1976].

[10] The Adamello pluton consists of ten major intrusive bodies [Bianchi *et al.*, 1970; Callegari and Dal Piaz, 1973]. True intrusion ages are available for the southernmost part only (Re di Castello massif, dated at 43–39 Ma by U/Pb on zircon [Hansmann and Oberli, 1991]. Rb/Sr, K/Ar and Ar/Ar-cooling ages on white mica, biotite and hornblende indicate progressive cooling from 42 Ma in the south to 29 Ma in the north [Del Moro *et al.*, 1983]. The study area near the Tonale fault zone comprises two of these intrusive bodies (Figure 2): the Avio intrusion in the west and the Presanella intrusion in the east. The Avio intrusion consists

of biotite quartz diorite, leucotonalite, biotite tonalite, including separate small gabbro complexes. K/Ar, Rb/Sr-cooling ages on biotite range between  $35.2 \pm 1.4$  and  $32.2 \pm 1.0$  Ma [Del Moro *et al.*, 1983]. The Presanella intrusion consists almost entirely of hornblende-tonalite. K/Ar, Rb/Sr-cooling ages on biotite and muscovite range from  $33.2 \pm 1.8$  to  $29.4 \pm 2.4$  Ma [Del Moro *et al.*, 1983]. Both these intrusions are characterized by a 1–2 km wide northern margin exhibiting a magmatic foliation oriented subparallel to the intrusive contact with the country rocks (Figure 3) [Bianchi *et al.*, 1970; Mendum, 1976; Werling, 1992]. This foliation crosses and hence postdates, the contact between the Avio and Presanella intrusions [Mendum, 1976], suggesting that their emplacement and crystallization overlapped in age.

[11] The strike of the Edolo schists, contact metamorphosed by Avio quartz diorite and Presanella tonalite,

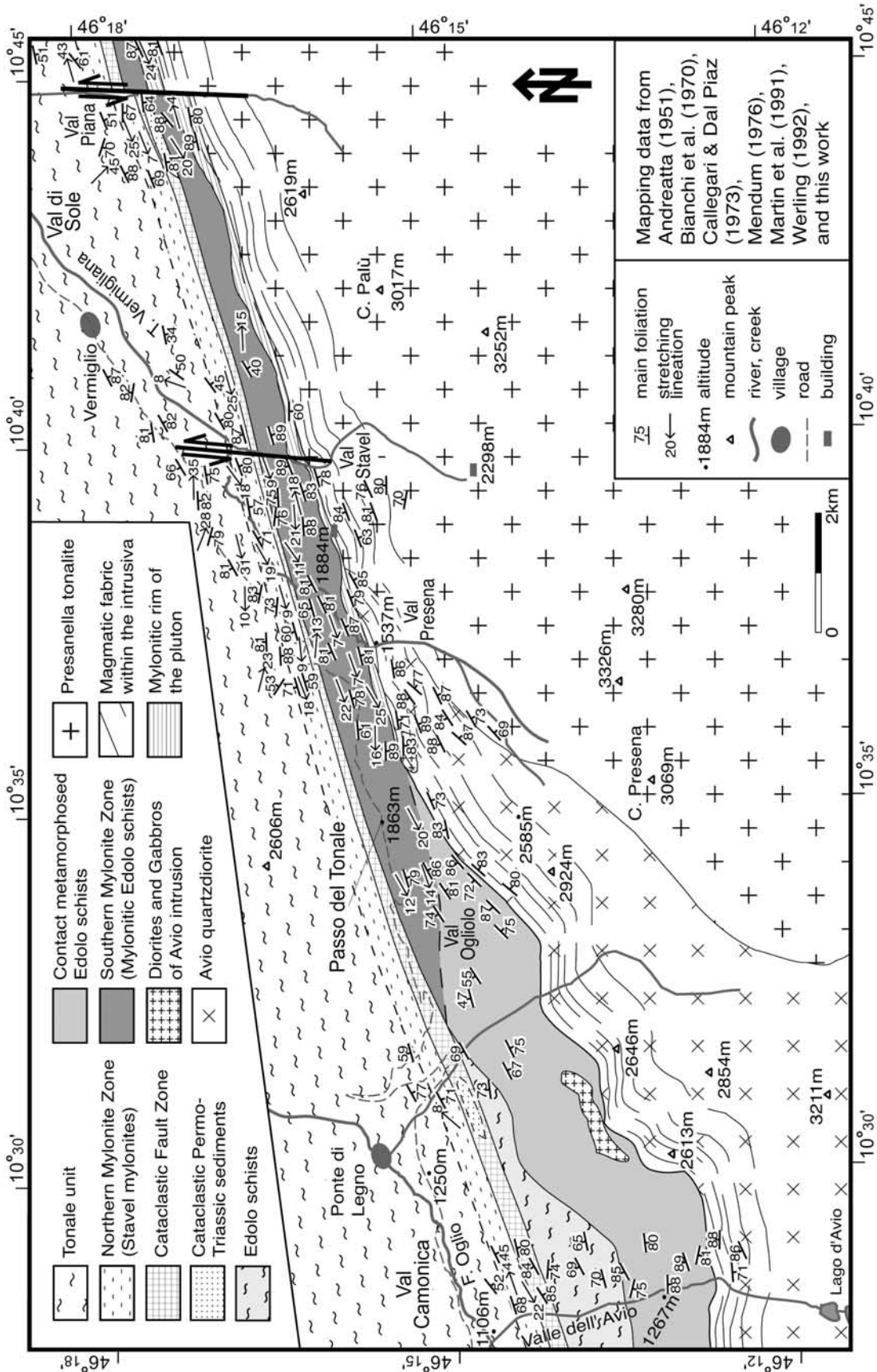
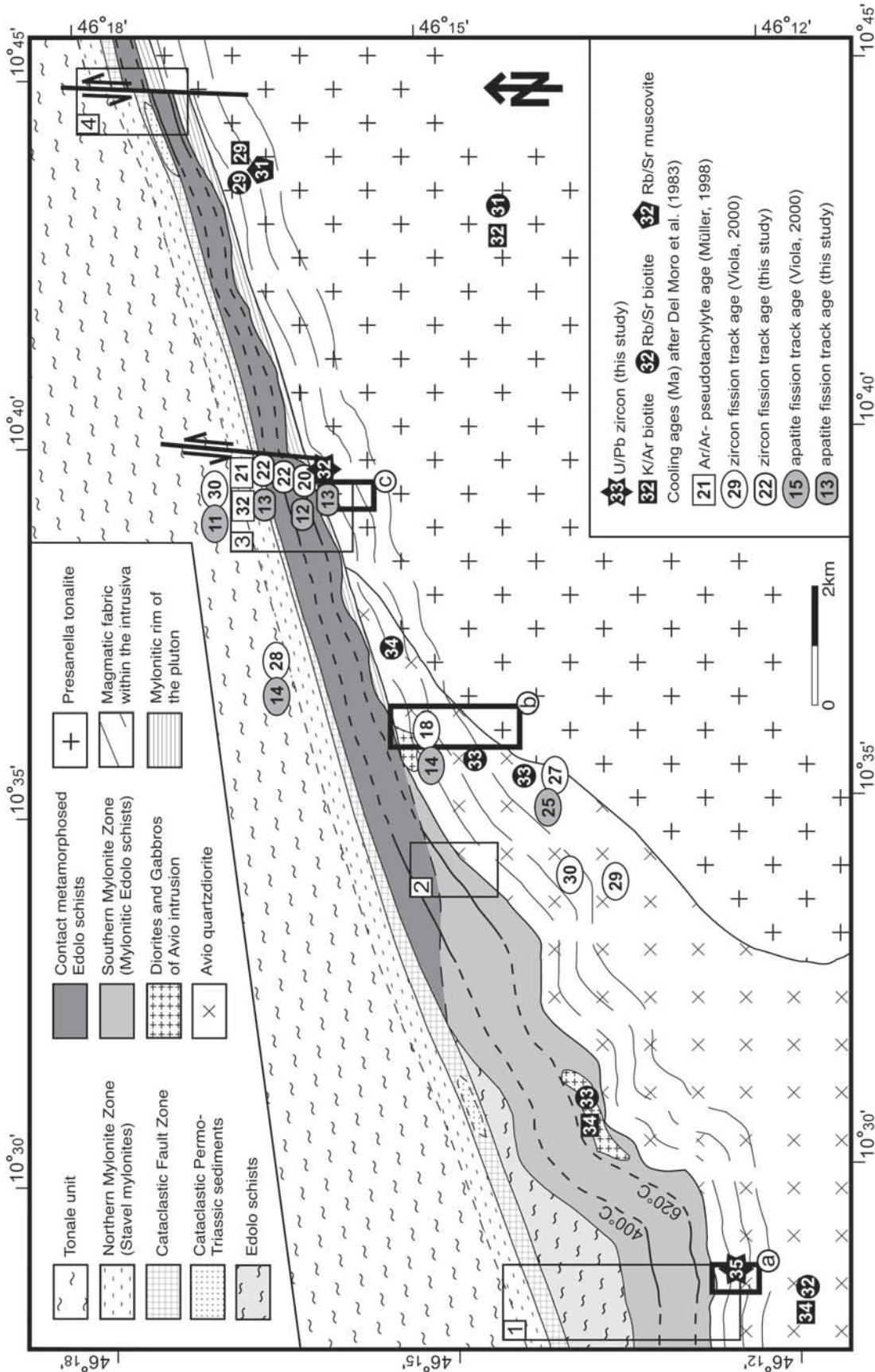


Figure 2. Simplified geological map of the area of study, showing representative measurements of main foliation and stretching lineation within the units affected by the deformation.



**Figure 3.** Area of study showing four sections mapped in detail (1, Valle dell'Avio; 2, Val Ogiolo; 3, Val Stavel; 4, Val Piana) and trend of the 400°C and 620°C isotherms of the Adamello contact aureole interpolated between these four sections (cf. Figures 6, 9, and 10). Solid lines represent the reaction isograds derived from mineral reactions; dashed lines represent the interpolation. Areas outlined with thick solid lines indicate the location of strain profiles derived from the shape of enclaves within the foliated rim of the Adamello pluton (a, Valle dell' Avio; b, Val Presena; c, Val Stavel). The locations of age data quoted from the literature are also indicated. Samples dated in this study are located more precisely in the detailed map sections of Figures 6 and 9.

**Table 1.** Data of U/Pb Analyses From Avio Quartz Diorite (Sample MS98-24.1) and Presanella Tonalite (Sample MS97-67.2)<sup>a</sup>

	Length, $\mu$	Aspect Ratio	U, ppm*	Pb, ppm*	<sup>206</sup> Pb/ <sup>204</sup> Pb		<sup>206</sup> Pb/ <sup>238</sup> U	<sup>207</sup> Pb/ <sup>235</sup> U	<sup>206</sup> Pb/ <sup>238</sup> U Age, Ma	<sup>207</sup> Pb/ <sup>235</sup> U Age, Ma	<sup>207</sup> Pb/ <sup>206</sup> Pb Age, Ma
					Measured	<sup>206</sup> Pb/ <sup>238</sup> U					
<i>Sample MS98-24.1</i>											
z2 1 prism	100	3:01	168.25	0.9227	170.84	0.00562 ± 17	0.0370 ± 29	36.1 ± 1.1	36.9 ± 2.9	89.7 ± 167	
z3 1 prism	400	4:01	713.31	3.9585	745.7	0.00555 ± 4	0.0362 ± 7	35.7 ± 0.3	36.1 ± 0.7	64.5 ± 41	
z4 5 prisms	100	4:01	401.01	2.1626	550.9	0.00546 ± 7	0.0359 ± 12	35.1 ± 0.5	35.8 ± 1.2	85.0 ± 72	
z5 5 prisms	150	4:01	819.22	7.9426	1754.3	0.00931 ± 4	0.0745 ± 6	59.7 ± 0.3	73.0 ± 0.6	531.6 ± 16	
<i>Sample MS97-67.2</i>											
z1 1 prism	150	3:01	117.41	0.8645	256.6	0.00741 ± 32	0.0569 ± 55	47.6 ± 2.1	56.1 ± 5.4	439.1 ± 1.2	
z2 2 prisms	100	3:01	134.42	0.7069	100.94	0.00514 ± 24	0.0344 ± 46	33.0 ± 1.5	34.3 ± 4.6	124.1 ± 285	
z3 3 prisms	75	3:01	110.4	0.5681	175.34	0.00508 ± 33	0.0324 ± 56	32.6 ± 2.2	32.4 ± 5.6	12.1 ± 370	
z4 5 prisms	100	2:01	130.41	0.6848	435.91	0.00541 ± 6	0.0364 ± 10	34.8 ± 0.4	36.3 ± 1.0	137.6 ± 56	

<sup>a</sup>Sample MS98-24.1 (longitude, 10°29'02"; latitude, 46°12'51"; Valle dell'Avio, Figure 9), sample MS97-67.2 (longitude, 10°39'10"; latitude, 46°15'53"; Val Stavel, Figure 6). Sample preparation followed standard procedures of bomb dissolution in a HF-HNO<sub>3</sub> mixture, and of HCl-based ion exchange purification of Pb and U on AG1-X8 resin, and mass spectrometric analysis on a Finnigan MAT 261 using silica gel-phosphoric acid loads for Pb and HNO<sub>3</sub> loads for U. Measurements were made either statically (combined faraday and electron multiplier) or dynamically (electron multiplier), depending on ion signal strength. The U and Pb ppm values are based on uncertain (visually estimated) sample weights. All errors shown are 2 $\sigma$  errors of the mean error; absolute U/Pb ratios are corrected for fractionation, blank (5 pg Pb, 0.2 pg U), and common Pb.

respectively, is oriented subparallel to this magmatic foliation (Figure 2). West of Passo del Tonale, the Tonale fault zone is subdivided into a greenschist facies mylonite belt to the north (Northern mylonite zone) and a discrete cataclastic fault zone to the south (Figures 2 and 3). The Cataclastic fault zone delineates the contact between Austro-Alpine and South-Alpine units. The contact aureole of the Avio intrusion is situated south of (i.e., outside) the Tonale fault zone. At Passo del Tonale, however, Tonale fault zone and northern margin of the Adamello intrusion converge. Further east, contact metamorphism and contemporaneous deformation causes the formation of the Southern mylonite zone south of the Cataclastic fault zone [Werling, 1992]. The degree of synkinematic contact metamorphism in the Southern mylonite zone varies from the chl-zone adjacent to the Cataclastic fault zone in the north to sil-kfs-bearing assemblages at the magmatic contact in the south [Werling, 1992; Stipp *et al.*, 2002a]. Hence in the east the Tonale fault zone consists of two separate mylonite belts, separated by the Cataclastic fault zone (Figures 2 and 3).

### 3. Methods of Study

[12] Samples for microstructural analyses were commonly quartz veins from mylonites. Sections were cut normal to the foliation and parallel to the stretching lineation. Where a stretching lineation was absent, samples were cut parallel to the strike of the foliation and thus approximately parallel to the usual orientation of the stretching lineation found in the Tonale mylonites. Recrystallization microstructures of quartz were characterized and quartz texture measurements carried out according to methods outlined by Stipp *et al.* [2002a, 2002b].

[13] In order to better constrain intrusion ages at the rim of the Adamello pluton U/Pb zircon ages have been determined from samples taken near the northern contact of the Presanella tonalite and the Avio quartz diorite

(Figure 3). Individual zircon prisms were selected for analysis based on form, clarity, and freedom from inclusions (see Table 1 for further explanations of the methods).

[14] Apatite and zircon fission track analyses were carried out in order to establish cooling path and for dating exhumation of the Austro- and South-Alpine basement units under the influence of contact metamorphism. Sample preparation followed the methods described by Seward [1989], further technical details can be found in Table 2 and are also given by Fügenschuh *et al.* [1997].

## 4. Mylonites and Cataclasites of the Eastern Tonale Fault Zone

[15] Four reasonably well-exposed sections across the fault zone (Figure 3) allow reconstructing the structural relationships between the different units. The four sections are, from west to east, two small valleys on the southern side of upper Val Camonica (Valle dell'Avio and Val Ogliolo) and two tributaries of the Val di Sole (Val Stavel and Val Piana). These sections extend over approximately 25 km along strike of the Tonale fault zone. Further to the east, outcrops of the Tonale line are nearly absent.

### 4.1. Eastern Tonale Fault Zone and Its Protoliths

[16] The Northern mylonite zone is entirely contained within the Austro-Alpine Tonale unit, while the Southern mylonite zone is derived from Edolo schists and Adamello granitoids. The Cataclastic fault zone contains protoliths derived from both Alpine tectonic units [Werling, 1992; Stipp and Schmid, 1998]. Adjacent to the Tonale fault zone these protoliths display steeply inclined to vertical foliation planes (Figures 4a and 4b). These preferentially strike WSW-ENE, i.e., subparallel to the mylonites and catacla-

**Table 2.** Apatite and Zircon Fission Track Data<sup>a</sup>

	Apatite Fission Track Samples			Zircon Fission Track Samples		
	MS-26.3	MS-18.5	MS-67.1	MS-26.3	MS-13.2	MS-18.5
Altitude, m	1420	1530	1500	1420	1625	1530
Longitude, deg	10°39'13"	10°39'08"	10°39'10"	10°39'13"	10°39'00"	10°39'08"
Latitude, deg	46°16'19"	46°15'59"	46°15'53"	46°16'19"	46°16'09"	46°15'59"
Number of grains counted	20	14	15	17	20	9
Standard track density $\times 10^4 \text{ cm}^{-2}$ (counted)	100.6 (3089)	100.9 (3089)	100.3 (3089)	14.44 (2000)	14.56 (2000)	14.50 (2000)
$\rho_s \times 10^4 \text{ cm}^{-2}$ (counted)	28.67 (112)	55.02 (199)	26.47 (191)	203.6 (1025)	300 (782)	385.7 (183)
$\rho_i \times 10^4 \text{ cm}^{-2}$ (counted)	394.2 (1540)	821.9 (2973)	377.8 (2726)	232.8 (1172)	343.8 (896)	476.3 (226)
P ( $\chi^2$ ), %	99	44	96	41	13	51
Age, Ma ( $\pm 2\sigma$ )	13.0 $\pm$ 2.6	12.0 $\pm$ 1.8	12.5 $\pm$ 2.0	21.8 $\pm$ 2.2	22.2 $\pm$ 2.8	20.4 $\pm$ 4.4

<sup>a</sup>All samples have been treated using the external detector method. Standard, spontaneous ( $\rho_s$ ) and induced track density ( $\rho_i$ ) and respective number of counted tracks (in parenthesis) are given; values for the ( $\chi^2$ ) test after Galbraith [1981]. Zircon ages were calculated with a zeta value of 348 for dosimeter glass SRM612. Apatite ages were calculated with a zeta value of 357 for dosimeter glass CN5. All ages are "central ages" [Galbraith and Laslett, 1993]; errors are quoted as  $2\sigma$ . For further technical details see Fügenschuh and Schmid [2003].

sites of the Tonale fault zone (Figures 4c–4h). This suggests that a steep belt had existed before the Tonale fault zone accommodated dextral strike-slip motion.

#### 4.2. Northern Mylonite Zone

[17] The Northern mylonite zone represents the eastern extension of a greenschist facies mylonite belt ("Insubric line"), which can be traced from Locarno (Figure 1) [e.g., Fumasoli, 1974; Wiedenbeck, 1986; Fisch, 1989; Schmid *et al.*, 1989]. In the study area (Figure 2), the boundary between Northern mylonite zone and Cataclastic fault zone is sharp. To the north the Northern mylonite zone is separated from the unshaped basement of the Tonale unit by a several hundred meters wide transition zone, characterized by a northward decreasing density of anastomosing shear zones. West of Vermiglio these narrow dextral shear zones overprint earlier mylonites formed by S-side-up thrusting associated with nappe stacking [Müller, 1998; Viola, 2000].

[18] The Northern mylonite zone formed under middle to lower greenschist facies metamorphic conditions. Pre-existent mineral assemblages are replaced by sericite and chlorite, plagioclase decomposing to albite, sericite, and clinozoisite. The reaction products define the mylonitic foliation, together with interconnected layers of quartz. Dynamic recrystallization of quartz preferentially occurred by subgrain rotation recrystallization (Figure 5a). Assuming typical natural strain rates between  $10^{-14} \text{ s}^{-1}$  to  $10^{-12} \text{ s}^{-1}$  [e.g., Pfiffner and Ramsay, 1982], a deformation temperature of approximately 400°C can be inferred [cf. Stipp *et al.*, 2002b]. Shear bands, asymmetric  $\sigma$ -clasts, mica-fish (Figure 5a), as well as quartz and calcite c-axis fabrics, indicate a dextral shear sense [Stipp, 2001].

#### 4.3. Cataclastic Fault Zone and Late-Stage Brittle Sinistral Shears

[19] The Cataclastic fault zone is a 80–200 m wide zone, situated between the Northern mylonite zone to the north and either the Edolo schists or the Southern mylonite zone

in the south. At Monte Padrio the width of the Cataclastic fault zone reaches 600 m [Werling, 1992]. Most fault rocks of the Cataclastic fault zone are weakly consolidated cataclasites, with rock clasts embedded in a fine-grained matrix of chlorite and other sheet silicates. The Cataclastic fault zone postdates the Northern mylonite zone because it contains clasts of previously formed mylonites of the Northern mylonite zone at its northernmost margin. However, the Cataclastic fault zone contains no clasts of the mylonites of the Southern mylonite zone, except in the Val Piana section (area 4 in Figure 3). This indicates that the Cataclastic fault zone predominantly affects non-mylonitic Edolo schists. In Val Piana, the Cataclastic fault zone also contains Permo-Triassic sediments [cf. Cornelius and Furlani-Cornelius, 1928, 1930; Malaroda, 1952], representing the northernmost part of the South-Alpine rock sequence.

[20] Cataclastic shear planes are poorly defined and therefore difficult to measure. However, one set of shear planes (H in Figure 4f) is parallel to the mylonitic foliation of the Northern mylonite zone and the Southern mylonite zone. A second set ( $R_1$  in Figure 4f) strikes nearly E-W, in a Riedel-1-geometry with respect to the H-maximum. A third set of Riedel planes ( $R_2$  in Figure 4f) occurs only locally. The overall geometry indicates a dextral shear sense [Müller, 1998], as was reported elsewhere in the Cataclastic fault zone by [Werling, 1992], based on S-C-fabrics.

[21] The cataclasites in the Val Stavel section represent the brittle counterpart of the Southern mylonite zone across the frictional-viscous transition [Stipp *et al.*, 2002a]. Shear band fabrics in the mylonites grade into Riedel shears. Hence the border between Cataclastic fault zone and Southern mylonite zone is less clearly defined in comparison with the abrupt transition between Cataclastic fault zone and Northern mylonite zone in the north. The deformation temperature in the Cataclastic fault zone is below that inferred for the frictional-viscous transition, i.e., below 280°C [Stipp *et al.*, 2002a].

[22] Discrete brittle faults are not restricted to the Cataclastic fault zone. They locally overprint all tectonic units.

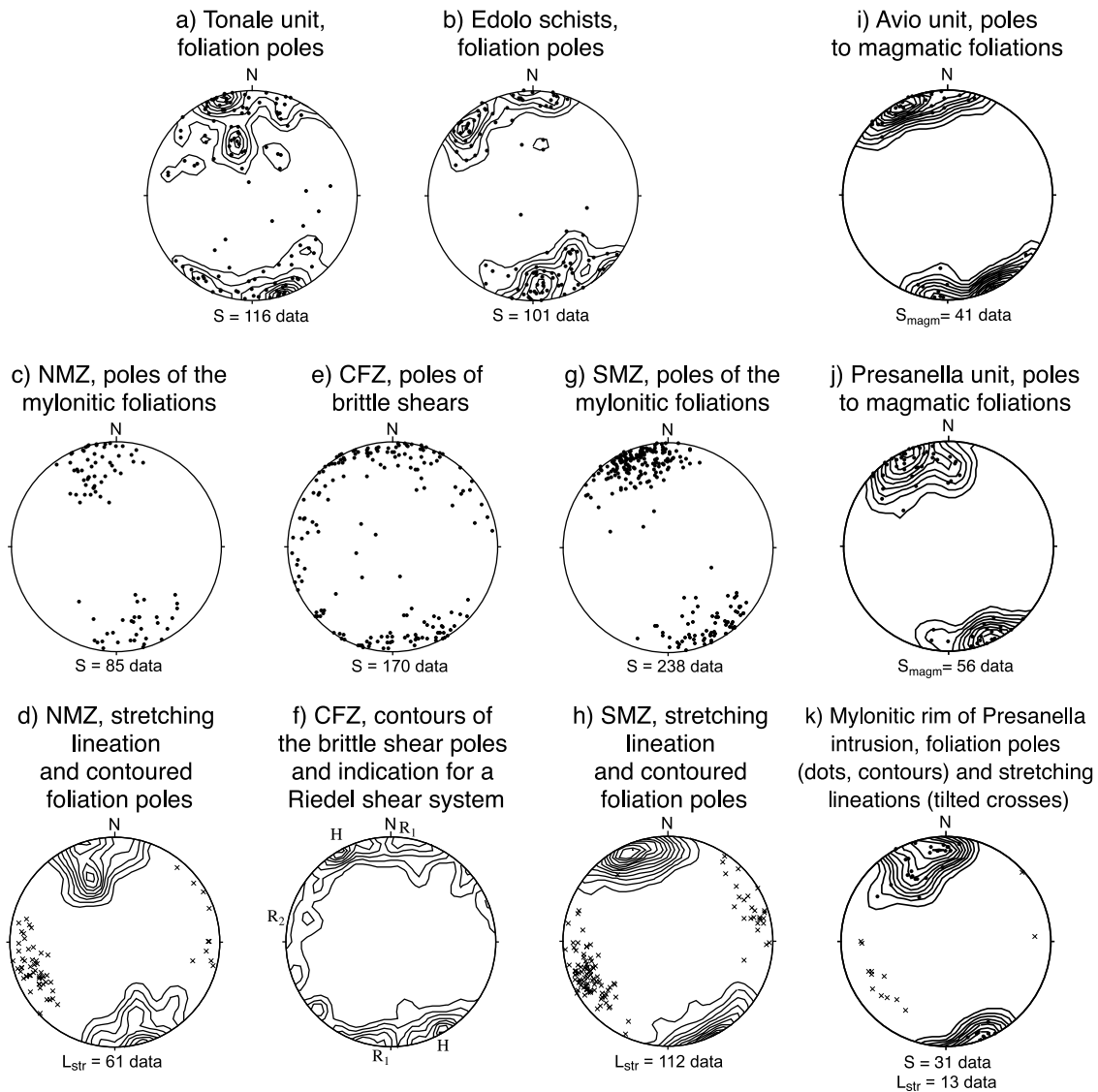


**Figure 4.** Compilation of planar and linear fabrics from the study area (cf. Figure 2). H, R<sub>1</sub>, R<sub>2</sub> in Figure 4f) are elements of a Riedel shear system proposed in the Valle dell' Avio section (see Figure 9) and discussed in the text. Abbreviations are as follows: CFZ, Cataclastic fault zone; NMZ, Northern mylonite zone; SMZ, Southern mylonite zone.

In particular, one sinistral, approximately N-S striking strike-slip zone clearly displaces all fault rocks by about 600 m near the eastern margin of Figure 2, and hence postdates the Tonale fault zone. Another sinistral shear is located to the west in Val Stavel [Mendum, 1976]. The strike of these late sinistral faults is sub-parallel to the Giudicarie line.

#### 4.4. Southern Mylonite Zone

[23] East of Passo del Tonale the 600 to 1000 m wide Southern mylonite zone, derived from the Edolo schists and situated between Cataclastic fault zone and Adamello pluton, formed due to a temperature increase caused by

the contact aureole of the syntectonic Presanella tonalite [Martin *et al.*, 1991; Werling, 1992; Stipp and Schmid, 1998]. A gradient of increasing temperatures, deduced from synkinematic mineral assemblages, is associated with changes in the mechanism of dynamic recrystallization of quartz (Figure 6) [Werling, 1992; Stipp, 2001; Stipp *et al.*, 2002a].

[24] Within 50 m of the contact with the Adamello intrusion, the Edolo schists contain large andalusite crystals, overgrowing corundum and sillimanite inclusions. The andalusite crystals are surrounded by a foliation formed by biotite, sillimanite (fibrolite), K-feldspar, plagioclase, and quartz. Therefore andalusite growth is interpreted as having outlasted the development of the main

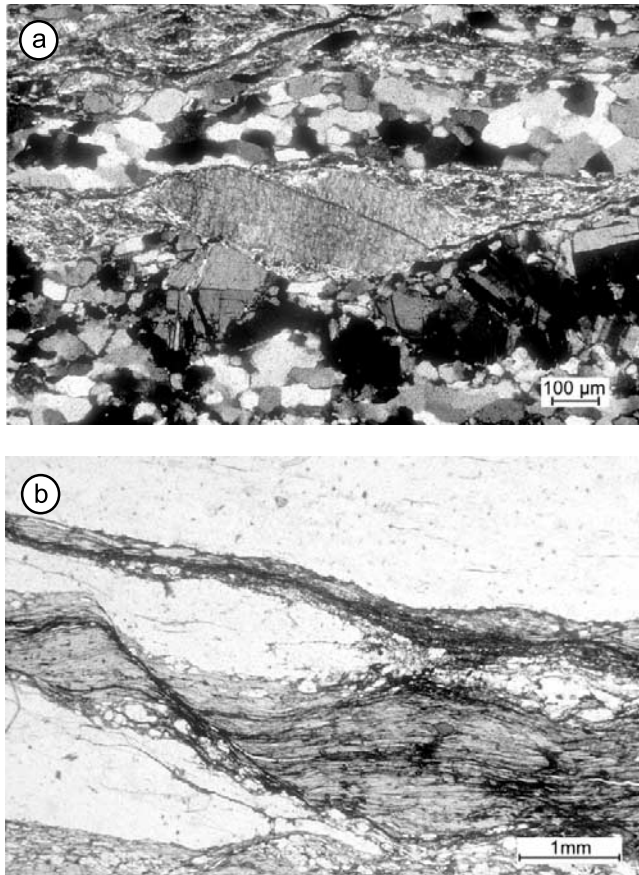


**Figure 5.** Dextral shear sense indicators from the two mylonite belts of the eastern Tonale fault zone (Northern and Southern mylonite zone) viewed perpendicular to foliation and parallel to stretching lineation. (a) Mica-fish in sericitic foliation; interconnected quartz layers display a recrystallized microstructure characteristic of subgrain rotation recrystallization with a grain size of approximately 50–80  $\mu\text{m}$ ; crossed polarized light. (b) Retrograde chlorite-bearing shear band in the biotite-muscovite zone of the Val Stavel section; plane polarized light.

sillimanite-bearing foliation. The presence of corundum ( $\geq 660^\circ\text{C}$  [cf. Stipp, 2001]) indicates that the metamorphic temperatures close to the contact exceeded those inferred from the minerals constituting the mylonitic foliation ( $\geq 620^\circ\text{C}$ ). Very high temperatures are also indicated by a migmatitic fabric in the mylonitic metasediments close to the magmatic contact: leucocratic portions display a microfabric of dispersed quartz, plagioclase, K-feldspar, and some randomly oriented biotite grains, indicating the presence of melt [e.g., Vernon, 1999]. After crystallization, the quartz grains have been partly overprinted by dynamic recrystallization, producing lobate and sutured grain boundaries and irregular, amoeboid, grain shapes. All these observations indicate temperatures around or above  $700^\circ\text{C}$  at the magmatic contact prior to the synkinematic mineral assemblages found in the Southern mylonite zone that

formed at temperatures above  $620^\circ\text{C}$  but below  $670^\circ\text{C}$  [Stipp *et al.*, 2002a].

[25] A dextral sense of shear in the Southern mylonite zone is mainly inferred from shear bands (Figure 5b) and texture analysis of synkinematic quartz veins (e.g., Figure 11h [Stipp *et al.*, 2002a]). Southwards, the Southern mylonite zone extends into the tonalite of the Presanella intrusion. There the plutonic rocks display a solid-state deformation associated with a mylonitic foliation and a stretching lineation parallel to those found in the Southern mylonite zone (Figures 4h and 4k) [Martin *et al.*, 1991; Stipp and Schmid, 1998].

## 5. Northern Margin of the Adamello Batholith

[26] Within 1 to 2 km of their northern margins, Avio quartz diorite and Presanella tonalite are foliated (Figures 2, 4i, and 4j) [Trener, 1906; Callegari and Dal Piaz, 1973]. The magmatic foliation is defined by the shape-preferred orientation of biotite and hornblende (Figure 7a) and mafic enclaves. The latter range in size between a few cm to some dm. The foliation becomes more penetrative towards the contact with the country rocks and cuts across the contact between the two intrusive bodies (Figure 3). Hence foliation formation postdates the final emplacement of the younger Presanella tonalite [Mendum, 1976]. Northern margin of the Avio unit and magmatic foliation both curve away from the Tonale fault zone west of Passo del Tonale (close to Val Ogliolo, area 2 in Figure 3) [Mendum, 1976; Werling, 1992]. This deflection suggests that west of Passo del Tonale, the marginal foliation of the Avio intrusion is produced by its emplacement only and is kinematically unrelated to dextral shear along the Tonale fault zone. This inference is supported by a lateral change in the inclination of the magmatic contact from near vertical (typical for the contact between Presanella tonalite and Southern mylonite zone) east of Passo del Tonale to a dip between  $60^\circ$ – $70^\circ$  to the NNW, typical for the contact between Avio quartz diorite and Edolo schists situated further to the west [Mendum, 1976]. Also, the width of the northern contact zone of the Adamello intrusion (i.e., the zone with magmatic injections inside the country rocks or, alternatively, pieces of wall rock incorporated as large xenoliths within the intrusion) increases from only 50–100 m east of Passo del Tonale to 200 m or more further west, indicating that the foliated margin was attenuated by the Tonale fault strike-slip displacements in the east only.

[27] The axial ratios of magmatic enclaves [Mendum, 1976; Werling, 1992; this work] (see Figure 8), measured along three cross sections normal to the magmatic contact (locations given in Figure 3), indicate that the strain ellipsoid becomes progressively more oblate toward the contact, which is consistent with a lack of a hornblende lineation within the foliation plane. Oblate strain ellipsoids indicate ballooning during the final emplacement of the intrusion [cf. Ramsay, 1989]. Thus a large part of the foliated margin of the younger Presanella intrusion formed

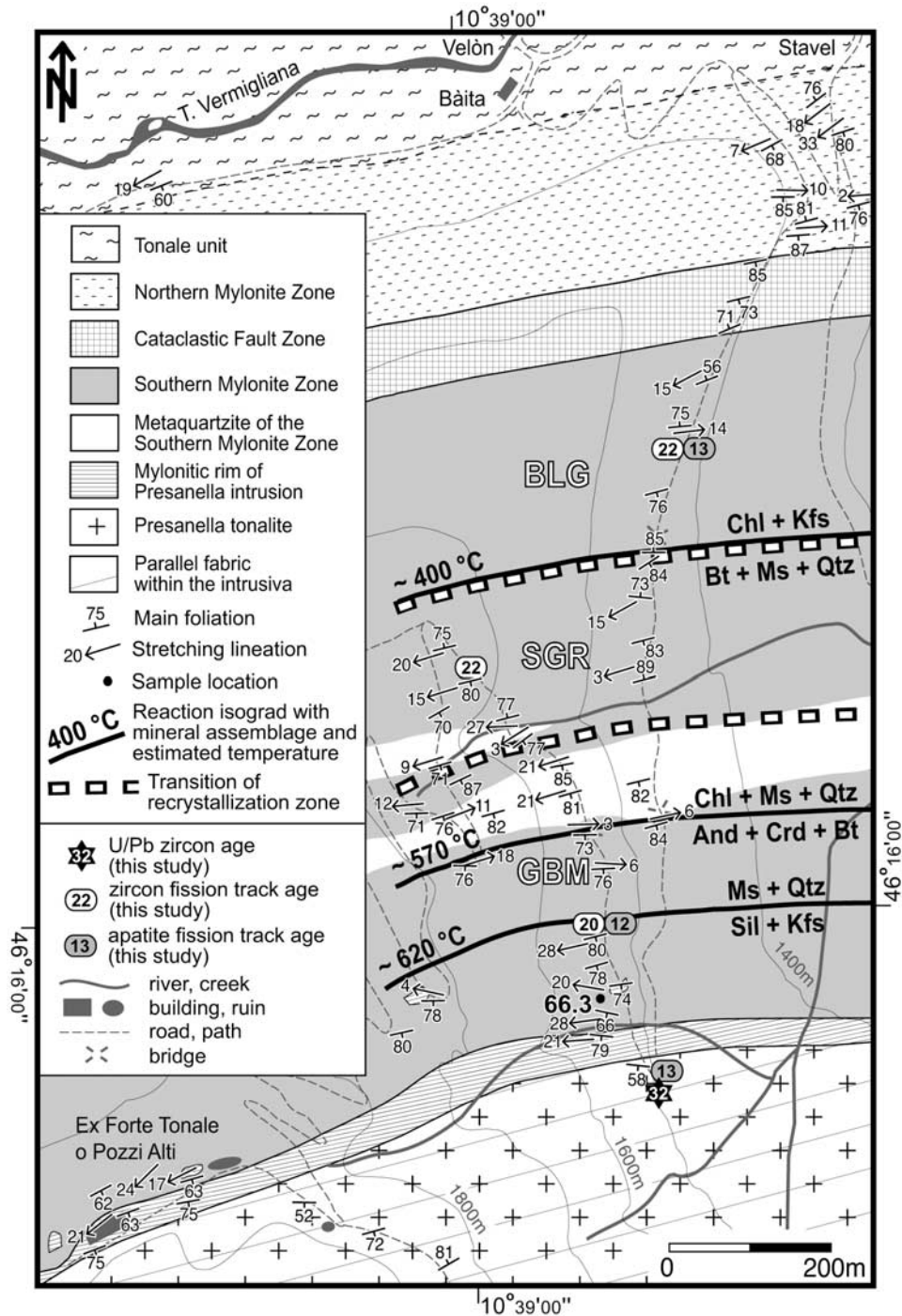


**Figure 6.** Map of the Val Stavel section. Abbreviations are as follows: BLG, zone of bulging recrystallization; SGR, zone of subgrain rotation recrystallization; GBM, zone of grain boundary migration recrystallization; for mineral reactions see *Stipp et al.* [2002a] (with permission from Elsevier Science). Locations of dated samples and their ages are indicated.

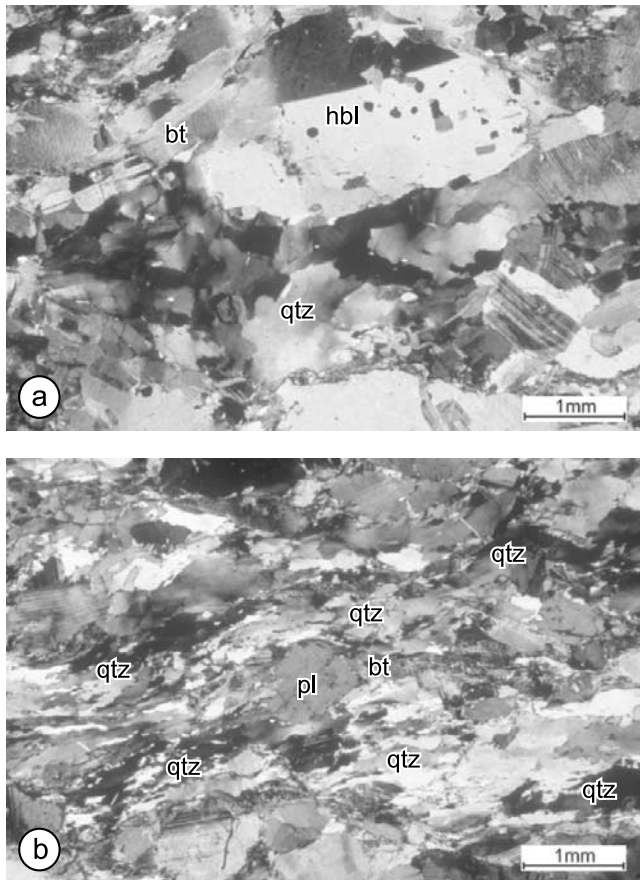


**Figure 7.** Micrographs of the foliated Presanella tonalite close to the contact with the Southern mylonite zone; crossed polarized light. Samples were taken close to the road bend in Val Stavel (location of 32 Ma age in Figure 6). (a) Magmatic hbl-bt foliation and a pocket of quartz displaying relatively large grain sizes and lobate grain boundaries of wide amplitudes (weakly deformed tonalite). Quartz microstructure is characteristic of grain boundary migration recrystallization at very high temperatures; sample orientation perpendicular to the foliation and parallel to the strike of the foliation. (b) Mylonitic foliation of solid state deformed tonalite from the contact to the Southern mylonite zone. Hbl is decomposed, the foliation is made up of biotite and interconnected weak layers of quartz. Quartz displays a grain boundary migration recrystallization microstructure with smaller grains (higher differential stress) than in Figure 7a and finely sutured grain boundaries pointing to a lower deformation temperature (retrograde metamorphic conditions). Sample orientation is normal to the foliation and parallel to the stretching lineation; dextral shear sense.

by ballooning. Possibly, this ballooning also partially affected the previously emplaced Avio quartz diorite (see discussion below).

[28] Superposed onto the magmatic foliation, a solid-state mylonitic foliation formed along the outermost rim of the Presanella tonalite in a 20 m to 300 m wide zone

[Martin *et al.*, 1991; Stipp and Schmid, 1998]. This foliation is defined by biotite and interconnected weak layers of quartz (Figure 7b). Solid-state deformation and dextral shear is indicated by quartz c-axis fabrics (e.g., sample 21.4 in Figure 13b of Stipp *et al.* [2002a]) and asymmetric  $\sigma$ -clasts (plagioclase in Figure 7b). Hornblende is commonly replaced by biotite and plagioclase, but oriented subparallel to the stretching lineation where preserved. The orientation of foliations and stretching lineations is indistinguishable from that observed in the adjacent Southern mylonite zone (Figures 2, 4h, and 4k). Thus this mylonitic solid-state overprint is associated with strike-slip movements along the Tonale fault zone, initiating after emplacement of the Presanella intrusion.

## 6. Relationships Between Contact Metamorphism and Deformation in the Contact Aureole of the Adamello Pluton

[29] From east (Val Piana) to west (Valle dell'Avio) the distance between Tonale fault zone and contact aureole of the Adamello pluton increases (Figure 3). In the contact aureole to the west (Figures 3 and 9) the Southern mylonite zone is absent, the pre-Alpine foliation of the Edolo schists is in its original orientation, and, pre-Alpine folding is preserved [cf. Stipp, 2001]. In a transitional area (Val Ogliolo; Figures 3 and 10), the Southern mylonite zone is still present but separated from the contact with the Adamello pluton by non-mylonitic contact metamorphosed Edolo schists. The latter section exhibits a continuous transition from the Southern mylonite zone to the contact metamorphosed Edolo schists, the stretching lineations

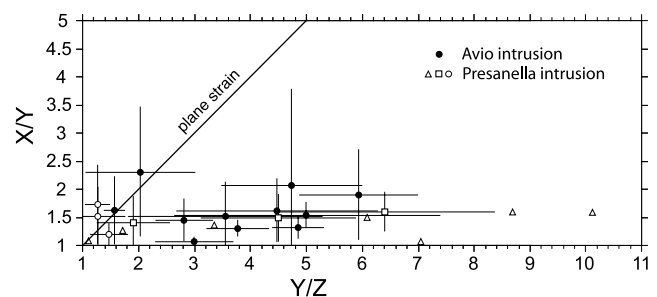


**Figure 8.** Flinn diagram for mafic enclaves compiled from three sections across the northern rim of the Adamello pluton (Valle dell'Avio, Val Presena, Val Stavel; see Figure 3 for section location). Each data point represents the mean of 10 to 29 enclaves from each locality. Open triangles (Presanella tonalite) represent data points from Mendum [1976]; open squares (Presanella tonalite) are from Werling [1992]; solid dots (Avio quartz diorite) and open dots (Presanella tonalite) are from this study. Error bars are 1 standard deviation. The XY plane is parallel to foliation, Z represents the foliation normal. Flattening decreases with increasing distance from the contact to the South-Alpine basement rocks toward the magmatic body. For further explanation see text.

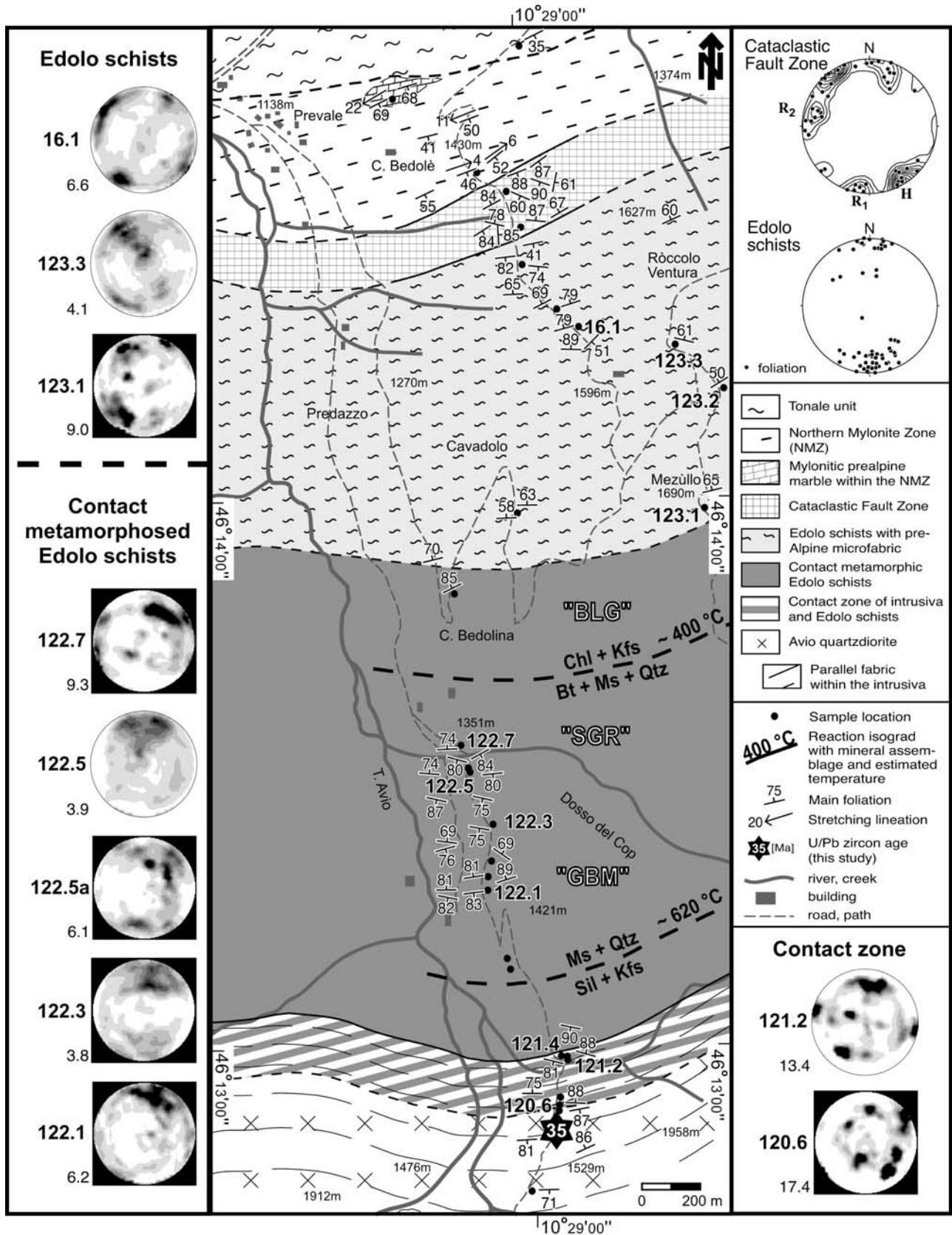


Figure 9

typical for the Southern mylonite zone progressively disappearing to the south and into the contact metamorphosed Edolo schists. Hence, in the west the contact metamorphosed Edolo schists preserve their pre-Alpine structures in the area between Cataclastic fault zone and Adamello pluton, whereas towards the east the Tonale mylonites (Southern mylonite zone) deform this same contact aureole. In the Stavel section (Figures 3 and 6) and further to the east, the Southern mylonite zone obliterated most pre-Alpine fabrics. The microstructural and textural transition from non-mylonitic to mylonitic Edolo schists (Southern mylonite zone) described below will be the basis for conclusions concerning the effects of strike-slip motion along the Tonale Fault zone during contact metamorphism.

### 6.1. Quartz Microfabrics of Pre-Alpine and Contact-Metamorphic Edolo Schists

[30] Edolo schists lacking contact metamorphism and/or deformational overprint are found in the northern part of the Valle dell'Avio section (Figures 3 and 9). Pre-Alpine quartz microstructures show largely annealed, fairly isometric grains with straight grain boundaries and coarse grain size (Figure 11a). Occasionally, a second pre-Alpine microstructure with large irregular grains and lobate boundaries is observed as well [cf. *Stipp*, 2001]. The textures display strong c-axis maxima close to the periphery of the pole figure (samples 16.1 and 123.1 in Figure 9) or incomplete girdle fabrics (sample 123.3 in Figure 9).

[31] Contact metamorphosed non-mylonitic Edolo schists are found in the southern part of the Valle dell'Avio section (Figure 9). The transition into these contact metamorphosed Edolo schists is gradual, and their northern boundary is difficult to map. Since the mineral assemblages are only partly equilibrated, reaction isograds are ill defined. Pre-Alpine quartz microstructures from within the lower temperature part of the contact aureole are only locally affected by a weak overprint. Even at temperatures above 400°C, large pre-Alpine porphyroclasts are still preserved. Recrystallization by subgrain rotation (SGR) is incomplete with large grains (70–300 μm; Figure 11b). At temperatures above 500°–550°C, all pre-Alpine relict microstructures disappear. Microstructural domains of equant grains with straight grain boundaries and 120° triple junctions suggest static recrystallization (Figures 11c and 11d).

[32] The textures of the contact metamorphosed Edolo schists in Valle dell'Avio (samples 122-7 to 122-1 in Figure 9) are similar to those of the original Edolo schists. C-axis pole figures measured by CIP and calculated from X-ray goniometry on higher temperature samples from the contact aureole in Valle dell'Avio largely represent the preferred orientation of recrystallized grains (samples 122-5 to 122-1 in Figure 9). The maxima are distributed in various patches on the crossed girdle fabric skeleton, possibly indicating static grain growth after deformation. In Valle dell'Avio the textural and microstructural development is in contrast with that observed further east (Val Stavel). There, changes in recrystallization mechanism in function of increasing temperatures coincide with systematic changes in the texture [*Stipp et al.*, 2002a, Figure 13]. The textures and microstructures in the Valle dell'Avio, however, indicate moderate strains during, and annealing after the emplacement of the Adamello batholith, i.e., strains which were insufficient to completely reset the pre-Alpine textures, as is the case in the Southern mylonite zone (compare Figures 10 and 11).

[33] The magmatic contact consists of a 200 m wide zone where migmatitic Edolo schists and the Avio quartz diorite are intercalated (Figures 9 and 10). The quartz textures from this contact zone (samples 121-2, 120-6 in Figure 9 and sample 100-1 in Figure 10) deviate from the pre-Alpine textures displaying strong single crystal maxima related to the large recrystallized grain size.

### 6.2. Quartz Microfabrics of Progressively Deformed Contact Metamorphic Edolo Schists

[34] Microfabrics of the contact metamorphosed Edolo schists in the southern part of the Val Ogliolo section indicate rather moderate deformation. Since a stretching lineation could not be observed, these rocks were classified and mapped as non-mylonitic contact metamorphosed Edolo schists. These less deformed Edolo schists south of the Southern mylonite zone (Figure 10) exhibit dynamic recrystallization microstructures of quartz. Very lobate grain boundaries indicate high temperature deformation during contact metamorphism (Figure 11g). This quartz microstructure (Figure 11g) corresponds to the GBM II recrystallization, described for the high temperature part of the GBM zone in the Val Stavel section (Figure 11h) [*Stipp et al.*, 2002a]. However, in the Val Ogliolo section some static

**Figure 9.** Map of the Valle dell'Avio section. Two pole figures on the right present field data of different tectonic units: The “foliations” are brittle shears in the Cataclastic fault zone and main foliations ( $S_0$ ) in the Edolo schists. Since there is no systematic difference in orientation between contact metamorphosed and non-contact metamorphosed Edolo schists, the data have not been separated in the diagram. In the pole figure for the Cataclastic fault zone the inferred Riedel shear system is indicated (H, main fault;  $R_1$ , synthetic Riedel shear;  $R_2$ , antithetic Riedel shear). Abbreviations are as follows: “BLG”, microstructures typical of bulging recrystallization; “SGR”, microstructures typical of subgrain rotation recrystallization; “GBM”, microstructures typical of grain boundary migration recrystallization; for mineral reactions, see *Stipp et al.* [2002a]. Locations of age dating samples and their ages are indicated. The [c]-axis pole figures from Computer Integrated Polarization (CIP) microscopy [*Panozzo Heilbronner and Pauli*, 1993](circles) and X-ray goniometry (circles with rectangular black frames) contoured in 0.5 intervals up to 4x uniform, sample numbers (on the left) and measured maxima (below, at the lower left corner) are indicated; the letter “a” in sample numbers indicates pole figures of smaller sections representing more localized textures (fabric domains). Pole figures are oriented normal to the foliation and parallel to the strike of the foliation.

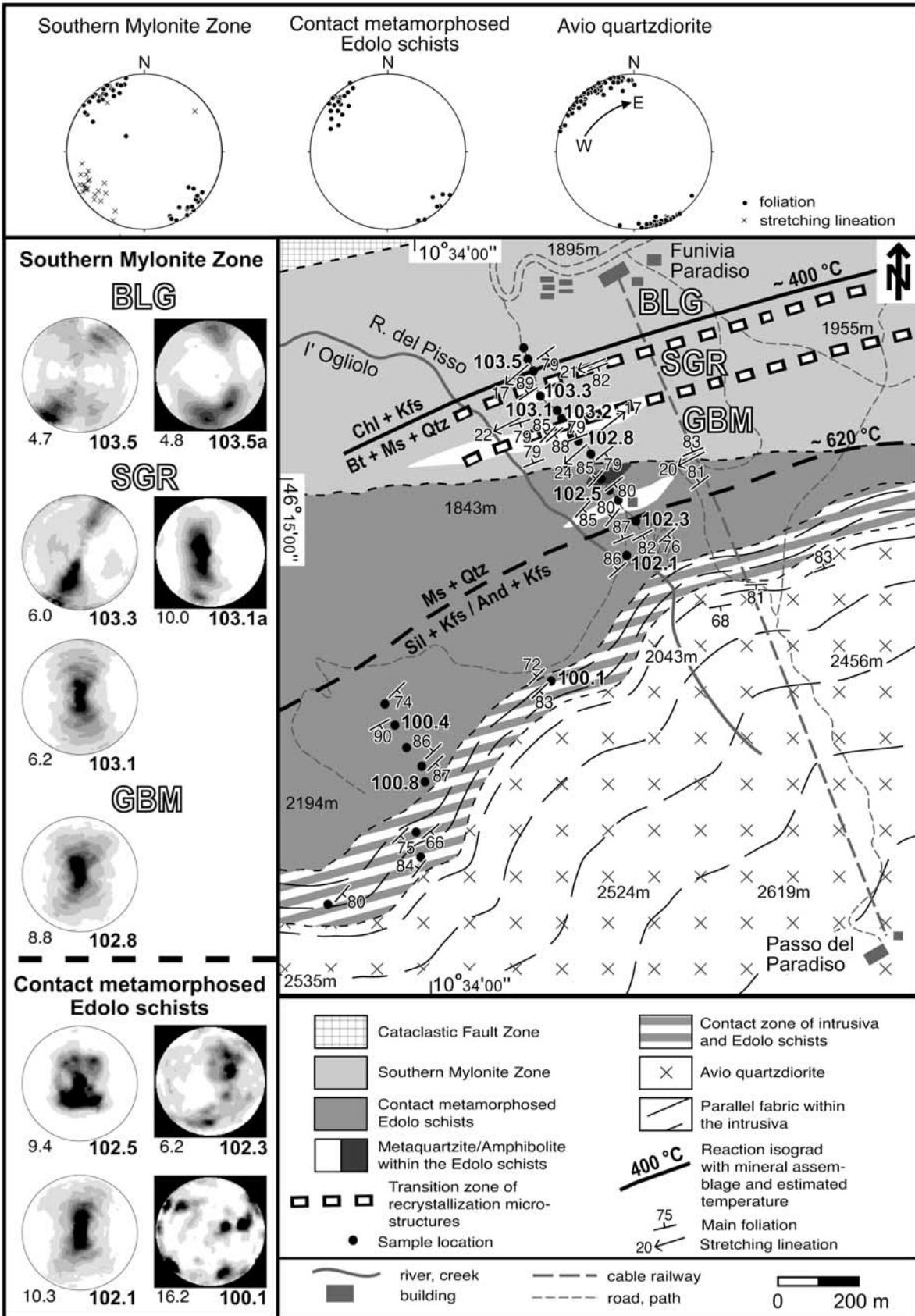


Figure 10

recrystallization of the microstructure occurs as well (Figure 11d).

[35] Further north and within the Southern mylonite zone, derived from Edolo schists, dynamic recrystallization microstructures of quartz exhibit with increasing temperature (profile between samples 103.5 and 102.8 in Figure 10): (1) bulging recrystallization (BLG; Figure 11e), (2) subgrain rotation recrystallization (SGR; Figure 11f), and (3) grain boundary migration recrystallization (GBM). The temperatures for these microstructural transitions were derived from synkinematic mineral assemblages (Figure 10), analogous to the situation in the Stavel section described by *Stipp et al.* [2002a].

[36] The textures in the Val Ogliolo section (Figure 10) are not as patchy as in the Valle dell'Avio section, indicating less annealing and more Alpine overprint (compare with Figure 9). Pole figures from the contact metamorphosed Edolo schists in the south usually display strong maxima subparallel to Y (samples 102-5, 102-1 in Figure 10), or resemble the pre-Alpine Edolo schists (sample 102-3 in Figure 10). In the mylonitic Edolo schists (Southern mylonite zone, samples 103.5 to 102.8 in Figure 10), i.e., at lower temperatures, bulk texture depends on the amount and the mechanism of dynamic recrystallization. Related c-axis pole figures are comparable to those from the Southern mylonite zone further east (Val Stavel section) [see *Stipp et al.* [2002a].

### 6.3. Effects of Strike-Slip Motion on Contact Metamorphism

[37] Figures 6, 9, and 10 demonstrate that the width of the contact aureole of the northern Adamello pluton narrows eastward, as it approaches the Tonale Fault Zone. This results in much more tightly spaced isotherms. This difference can not be attributed to differing heat fluxes associated with the Avio and Presanella intrusions, because the maximum temperatures at the rim of both intrusions are similar (700°–800°C) and because the Presanella tonalite is larger than the Avio quartz diorite in the west [*Bianchi et al.*, 1970; *Callegari and Dal Piaz*, 1973]. The Stavel section (Figure 6) provides particularly clear evidence for disturbance of the contact aureole because its temperature-distance function [*Stipp et al.*, 2002a, Figure 6] is linear rather than exponential, as is expected for an undisturbed contact aureole [e.g., *Buntebarth and Voll*, 1991; *Pattison and Harte*, 1991]. Modeling with the program CONTACT

[*Peacock*, 1989] using a one-dimensional heat flux array also predicts a nearly exponential decrease of temperature with increasing distance from the Presanella intrusion [*Stipp*, 2001]. Hence reduced width and linear temperature-distance function of the Presanella contact aureole require a structural explanation which will be given in the discussion section.

## 7. Age Constraints on the Cooling History

[38] We now present new age data, complemented by Rb-Sr and K-Ar age determinations from the literature. This allows a time frame to be established regarding the activity of the eastern Tonale fault zone.

### 7.1. Zircon U/Pb Ages

[39] Samples of the Presanella tonalite in Val Stavel (sample 67-2 in Figure 6) and the Avio quartz diorite in Valle dell'Avio (sample 24-1 in Figure 9) were taken very close to the northern contact of the Adamello intrusion. The U/Pb measurements on four fractions of zircon from each sample, each fraction containing 1 to 5 zircon prisms (Figure 12 and Table 1), range from concordant to moderately discordant. The lower and upper intercept ages are  $34.6 \pm 1.0$  Ma and  $1007 \pm 39$  Ma for the Avio quartz diorite (Figure 12a), and  $32.0 \pm 2.3$  Ma and  $1022 \pm 450$  Ma for the Presanella tonalite (Figure 12b). The concordant analyses in both samples cluster at the lower intercept ages, and they are interpreted to record the magmatic crystallization/emplacement ages of these plutons. The discordant analyses lie at older U/Pb ages, strongly suggesting they reflect inheritance from older crustal material. The upper intercept ages are therefore interpreted to record the presence of a minor component of crustal inheritance approximately 1 Ga in age, comparable to the 1.1 Ga age estimated from inherited zircon components in the Re di Castello unit of the Southern Adamello pluton [*Hansmann and Oberli*, 1991].

[40] The  $32.0 \pm 2.3$  Ma U/Pb zircon age from the Presanella tonalite in Val Stavel (Figure 6), in combination with the Rb/Sr-cooling age of muscovite (31 Ma) and the K/Ar- and Rb/Sr-cooling ages of biotite (32–29 Ma [*Del Moro et al.*, 1983]; Figure 3), indicates fast cooling below 300°C immediately after the intrusion (Figure 13). The  $34.6 \pm 1.0$  Ma U/Pb zircon age from the marginally older Avio granodiorite (Figure 9) and K/Ar- and Rb/Sr-cooling ages of 34 and 32 Ma, respectively for biotite (Figure 3)

**Figure 10.** Map of the Val Ogliolo section. Three pole Figures at the top present field data of different tectonic units: The “foliation” data are mylonitic foliations in the Southern mylonite zone, main foliations ( $S_0$ ) in the contact metamorphosed Edolo schists, and magmatic foliations within the Avio quartz diorite. The pole figure concerning the Avio quartz diorite displays a progressive clockwise rotation of the foliation in the Tonale pass area and also includes measurements taken by *Werling* [1992] south and southeast of Passo del Tonale and outside of the map area. Abbreviations are as follows: BLG, zone of bulging recrystallization; SGR, zone of subgrain rotation recrystallization; GBM, zone of grain boundary migration recrystallization; for mineral reactions see *Stipp et al.* [2002a]. The [c]-axis pole Figures from CIP (circles) and X-ray goniometry (circles with rectangular black frames) contoured in 0.5 intervals up to 4x uniform, sample numbers (below on the right) and measured maxima (below on the left) are indicated; the letter “a” in sample numbers indicates pole Figures of smaller sections representing more localized textures (fabric domains). Pole Figures are oriented normal to the foliation and parallel to the stretching lineation, or, if there is no stretching lineation, parallel to the strike of the foliation.

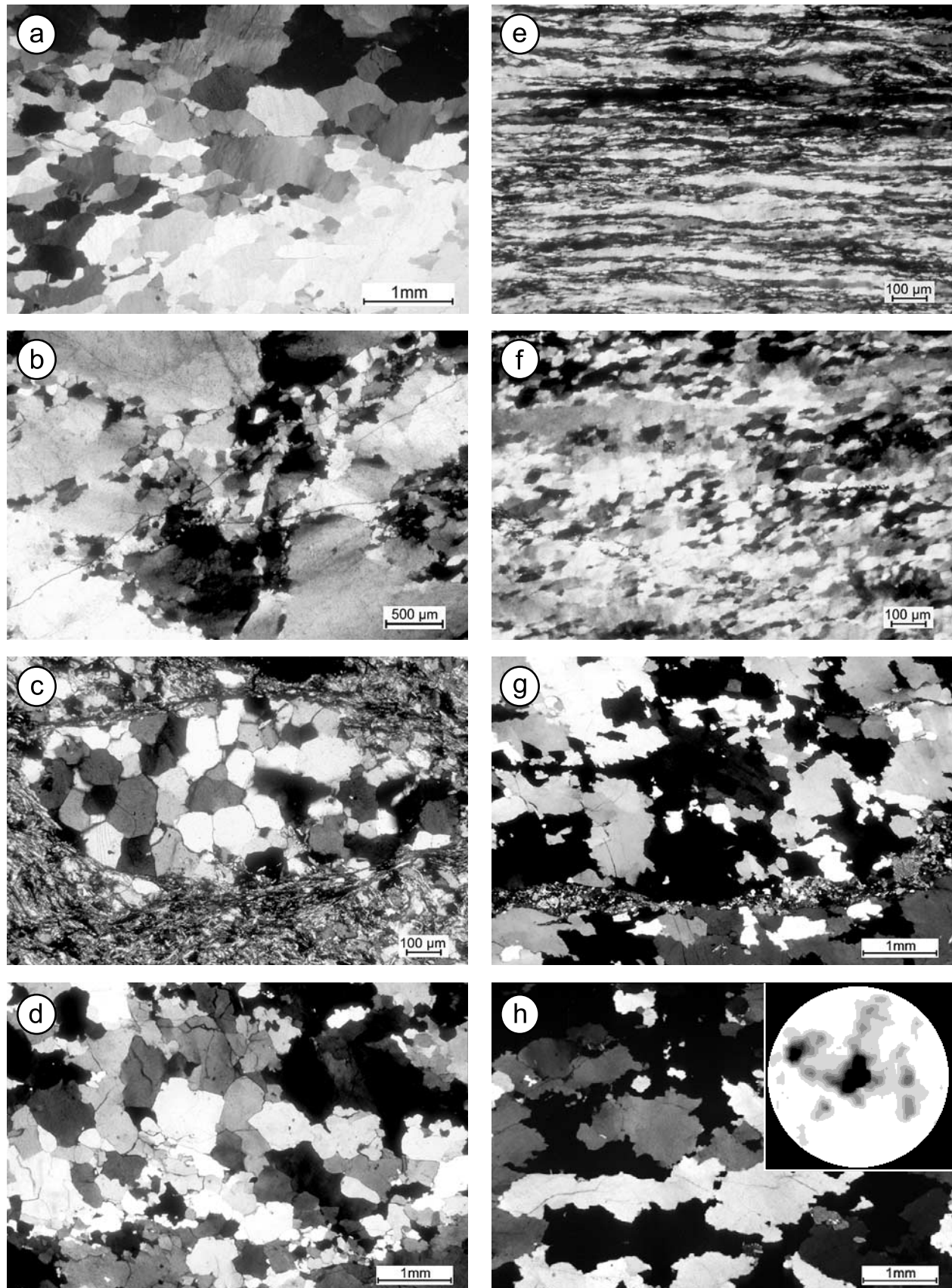


Figure 11

indicates that this intrusion was also subject to very fast cooling following emplacement.

## 7.2. Apatite and Zircon Fission Track Ages

[41] Four fission track samples were collected in the Val Stavel section (see Figure 6 for localities). Three are from the low ( $T_{\max} \approx 350^{\circ}\text{C}$ ; sample 26-3), intermediate ( $T_{\max} \approx 450^{\circ}\text{C}$ ; sample 13-2) and high ( $T_{\max} \approx 600^{\circ}\text{C}$ ; sample 18-5) temperature parts of the Southern mylonite zone, respectively. One is from the Presanella tonalite close to the contact (sample 67-1). Despite these differences in temperature all samples yielded consistent ages of 12–13 Ma (apatite) and 20–22 Ma (zircon), respectively (Figure 6 and Table 2). Since all samples have been taken from similar elevations, an altitude dependence of the ages can be excluded. Zircon and apatite fission track ages indicate slow cooling and exhumation of the South-Alpine units during the Miocene (Figure 13). The contact aureole around the Adamello intrusion fully annealed any pre-Oligocene fission tracks, while Cretaceous zircon fission track ages for the Edolo schists are found 5 km west of Edolo, i.e., outside the area of contact metamorphism [Viola, 2000].

[42] Zircon fission track ages of 30 and 28 Ma, respectively, are found in the Tonale unit east of the Tonale pass [Viola, 2000] (Figure 3). This indicates that cooling to temperatures below  $240^{\circ}\text{C}$  occurred earlier north of the eastern Tonale fault zone and in the Austro-Alpine basement rocks, and that the Austro-Alpine units were not affected by Adamello contact metamorphism. A zircon fission track age from the Avio quartz diorite (18 Ma) [Viola, 2000] (Figure 3), located close to the contact with the Edolo schists, agrees with the young zircon fission track ages from the Southern mylonite zone in the Val Stavel section. Three other samples from the Avio quartz diorite dated by Viola [2000], however, range between 27 to 30 Ma (Figure 3). These samples, situated further away from the intrusive contact and at a 500–1500 m higher altitude,

display a large scatter of the single grain ages, and they fail the chi-square test [Viola, 2000]. These features indicate slow overall cooling through the zircon partial annealing zone.

## 8. Summary and Discussion

### 8.1. Pluton Emplacement

[43] In contrast to the results of most other studies dealing with syntectonic magmatism [e.g., Davidson *et al.*, 1992; Brown and Solar, 1999; Andronicos *et al.*, 2003; Moya *et al.*, 2003], and in contrast to the findings regarding all the other intrusions aligned along the Periadriatic Fault System [e.g., Rosenberg, 2004], ascent and emplacement of the northern Adamello pluton did not take place within this simultaneously active fault system, nor was pluton emplacement directly related to dextral transpression along the adjacent Tonale fault zone. Also the earlier stages of pluton emplacement, observed in the southern Adamello, were not associated with regional tectonic activity within the Southern Alps [Schönborn, 1992], but took place by forceful intrusion [e.g., Brack, 1983; John and Blundy, 1993; John and Stünitz, 1997]. Ballooning related to the Presanella intrusion occurs contemporaneously with dextral shearing along the adjacent Tonale fault zone, as is indicated by high temperature mylonites ( $\sim 650^{\circ}\text{C}$ ) that formed under contact metamorphic conditions [Stipp *et al.*, 2002a] at the contact to both the Avio ( $34.6 \pm 1.0$  Ma) and the Presanella ( $32.0 \pm 2.3$  Ma) intrusion. No simultaneous shearing could be demonstrated regarding magmatic flow within the intrusives.

[44] Hence we conclude that the Tonale fault zone did not promote ascent, emplacement or exhumation of the northern Adamello pluton. Instead, this fault zone terminated the observed propagation of intrusions within the Adamello pluton towards the north. However, we cannot exclude that melt formation and ascent of the southern Adamello pluton

**Figure 11.** Characteristic quartz microstructures from Valle dell’Avio, Val Ogliolo, and Val Stavel sections produced at different temperatures of contact metamorphism and associated with or without intense straining; crossed polarized light. Specimen locations are given in Figures 9 and 10. (a) Pre-Alpine annealed recrystallization microstructure in the Edolo schists (Valle dell’Avio, sample 123.2, Figure 9). (b) SGR-microstructure from the contact metamorphosed Edolo schists: core and mantle structure of pre-Alpine porphyroclasts with subgrain rotation recrystallization. Recrystallized grains and subgrains are about the same size (recrystallized grain size  $\approx 100\text{--}200\ \mu\text{m}$ ; Valle dell’Avio, sample 122.7, Figure 9). (c) Clast in pelitic matrix showing static recrystallization: isometric grains with straight grain boundaries, triple junctions and absence of intracrystalline deformation features (Valle dell’Avio, sample 122.6, Figure 9). (d) Static recrystallization microstructure from the contact metamorphosed Edolo schists: isometric grains with straight grain boundaries and triple junctions with dihedral angles. Some more irregular grains with lobate grain boundaries (e.g., in the upper right corner) occur as well (Val Ogliolo, sample 100.4, Figure 10). (e) Zone of BLG (upper temperature part; BLG II from Stipp *et al.* [2002a]) in the Southern mylonite zone: Elongated porphyroclasts, sutured grain boundaries with bulges indicating dominant bulging recrystallization (Val Ogliolo, sample 103.3, Figure 10). (f) Zone of SGR (upper temperature part) in the Southern mylonite zone: ribbon grains are almost completely recrystallized by subgrain rotation recrystallization (recrystallized grain size  $\approx 50\ \mu\text{m}$ ; Val Ogliolo, sample 103.2, Figure 10). (g) GBM-microstructure (GBM II from Stipp *et al.* [2002a]) from the contact metamorphosed Edolo schists: amoeboid grains with large amplitude saturations, large recrystallized grain sizes and “dissection microstructures” (Val Ogliolo, sample 100.8, Figure 10). (h) Zone of GBM (upper temperature part; GBM II from Stipp *et al.* [2002a]) in the Southern mylonite zone: amoeboid grains with large amplitude saturations, very large recrystallized grain sizes and “dissection microstructures”; inserted quartz c-axis pole figure from Figure 13b of Stipp *et al.* [2002a] (with permission from Elsevier Science) (Val Stavel, sample 66.3, Figure 6).

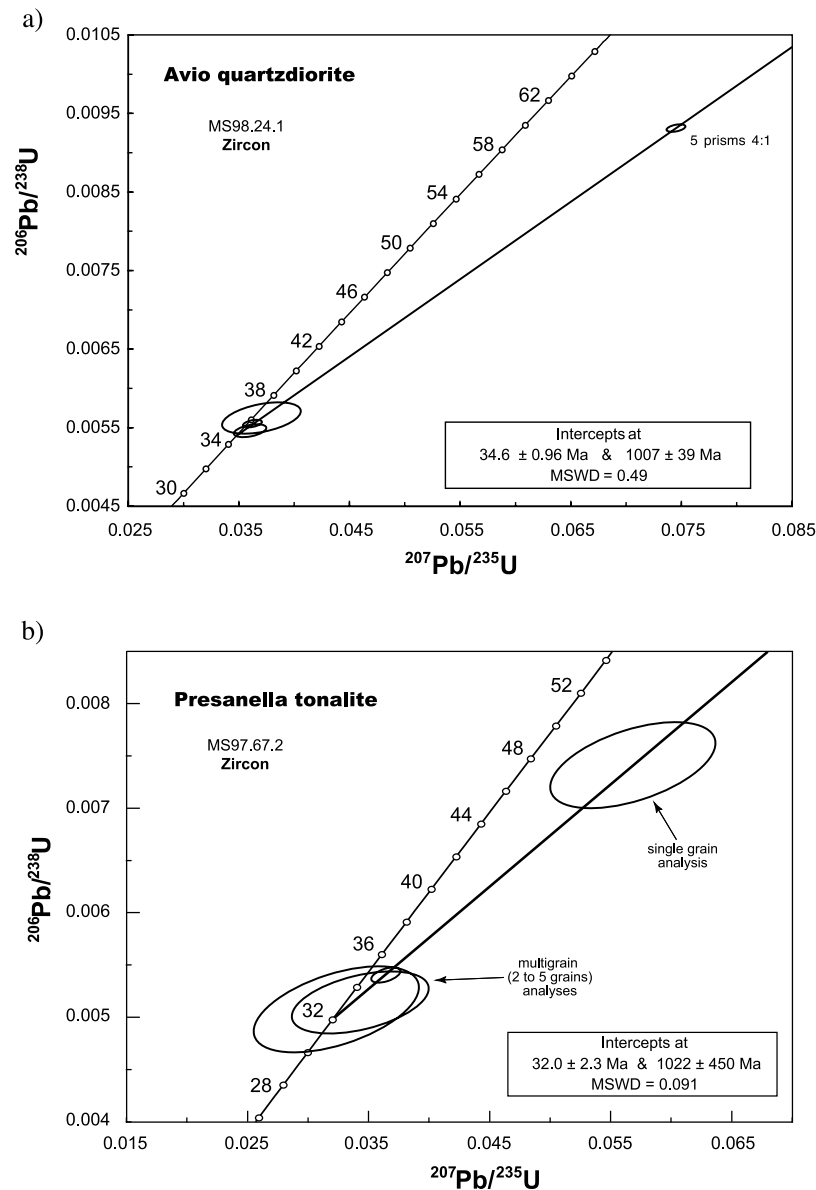


**Figure 12.** U/Pb diagrams of single zircon dating from (a) the Avio quartz diorite in Valle dell' Avio (sample MS98-24.1; see Figure 9 for sample location) and (b) the Presanella tonalite in Val Stavel (sample MS97-67.2; see Figure 6 for sample location).

could be related to the precursor of another segment of the Periadriatic Fault System, the Giudicarie line, situated east of the pluton. Schmid *et al.* [2003] postulate, on the basis of teleseismic tomography data of Lippitsch *et al.* [2003], that present-day subduction polarity changed from south directed in the Western to north directed in the Eastern Alps. Giudicarie line and Adamello pluton are located at this transition and magma ascent may have occurred along the deep fault zone delimiting the polarity change.

## 8.2. Thermal Evolution After Intrusion

[45] Cooling from peak contact metamorphic conditions, prevailing at 32 Ma (Presanella intrusion), to below the

Rb/Sr- and K/Ar-blocking temperatures of biotite ( $\approx 300^\circ\text{C}$ , [cf. Hunziker *et al.*, 1992]) at  $\sim 30$  Ma is fast and followed by slow cooling through the annealing temperature of zircon fission tracks (Figure 13). The initial stage of fast cooling to  $\sim 250^\circ\text{C}$  suggests that ambient temperatures before the Avio and Presanella intrusions were at around  $250^\circ\text{C}$ . This, together with pressures of around 2.5 kb, derived from contact metamorphic assemblages [Stipp *et al.*, 2002a], indicates a geothermal gradient of around  $26^\circ\text{--}27^\circ/\text{km}$ .

[46] According to Figure 13, the slow cooling rates during the second cooling stage slightly increased after about 22 Ma (zircon fission track). This probably reflects final exhumation during Miocene erosion, following post-Adamello thin-skinned thrusting within the Milan belt

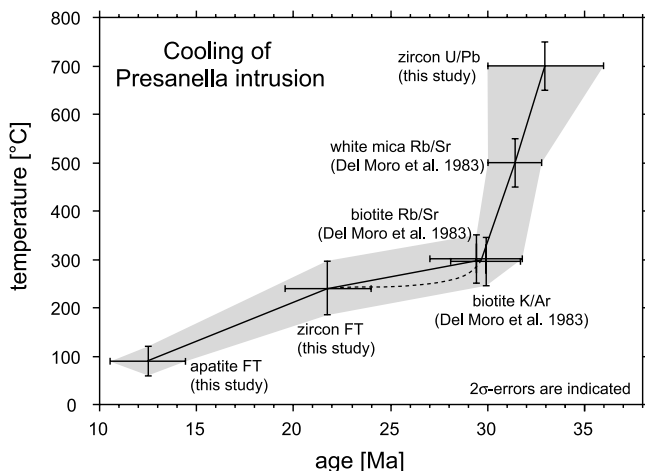


**Figure 13.** Temperature-time diagram for the Presanella intrusion and its contact aureole in the Val Stavel section. Blocking temperatures for the isotope systems are taken from *Hunziker et al.* [1992, and references therein]. Dashed line indicates supposed T/t path after cooling below temperatures required for mylonitization within the Southern mylonite zone. See text for further explanation.

[Schönborn, 1992], postdating dextral strike slip along the Tonale fault zone according to *Schmid et al.* [1996]. The apatite ages derived from our study (12–13 Ma) are in accordance with the 11–14 Ma age range from Tonale unit and Avio intrusion [*Viola, 2000*] (Figure 3). Only one sample from the Avio intrusion in Val Presena shows a much older apatite age (25 Ma [*Viola, 2000*]; Figure 3), which does not fit into the otherwise consistent regional pattern of apatite fission track ages.

### 8.3. Tectonic Evolution Along the Eastern Tonale Fault Zone

[47] Tectonic activity along the eastern Tonale fault zone starts with the formation of the Northern mylonite zone. The mylonites of the Northern mylonite zone postdate earlier formed “Steep Shear Zones” within the Tonale unit, dated by Rb/Sr on synkinematic white mica ( $36.8 \pm 5.1$  Ma [*Müller, 1998*] and by Ar/Ar stepwise-heating on fault-related pseudotachylytes ( $36.4 \pm 0.6$  Ma [*Müller, 1998*];  $35.0 \pm 0.8$  Ma [*Viola, 2000*]). Hence the formation of the Northern mylonite zone must be younger than about 36 Ma, but definitely older than 30 Ma, as is indicated by the zircon fission track ages from Tonale unit gneisses adjacent to the Northern mylonite zone (Figure 3) [*Viola, 2000*]. Furthermore, a crosscutting pseudotachylyte injection vein in an antithetic Riedel shear plane in the Val Stavel section, postdating the Northern mylonite zone, yields a laser ablation Ar/Ar age of  $32.1 \pm 3.5$  Ma [*Müller, 1998*].

[48] From the beginning of fault zone activity at ~35 Ma, the kinematics of movement along the eastern Tonale fault zone indicate dextral strike slip, combined with minor uplift of the northern block. This relative uplift allows for concomitant deformation of rocks across the frictional-viscous

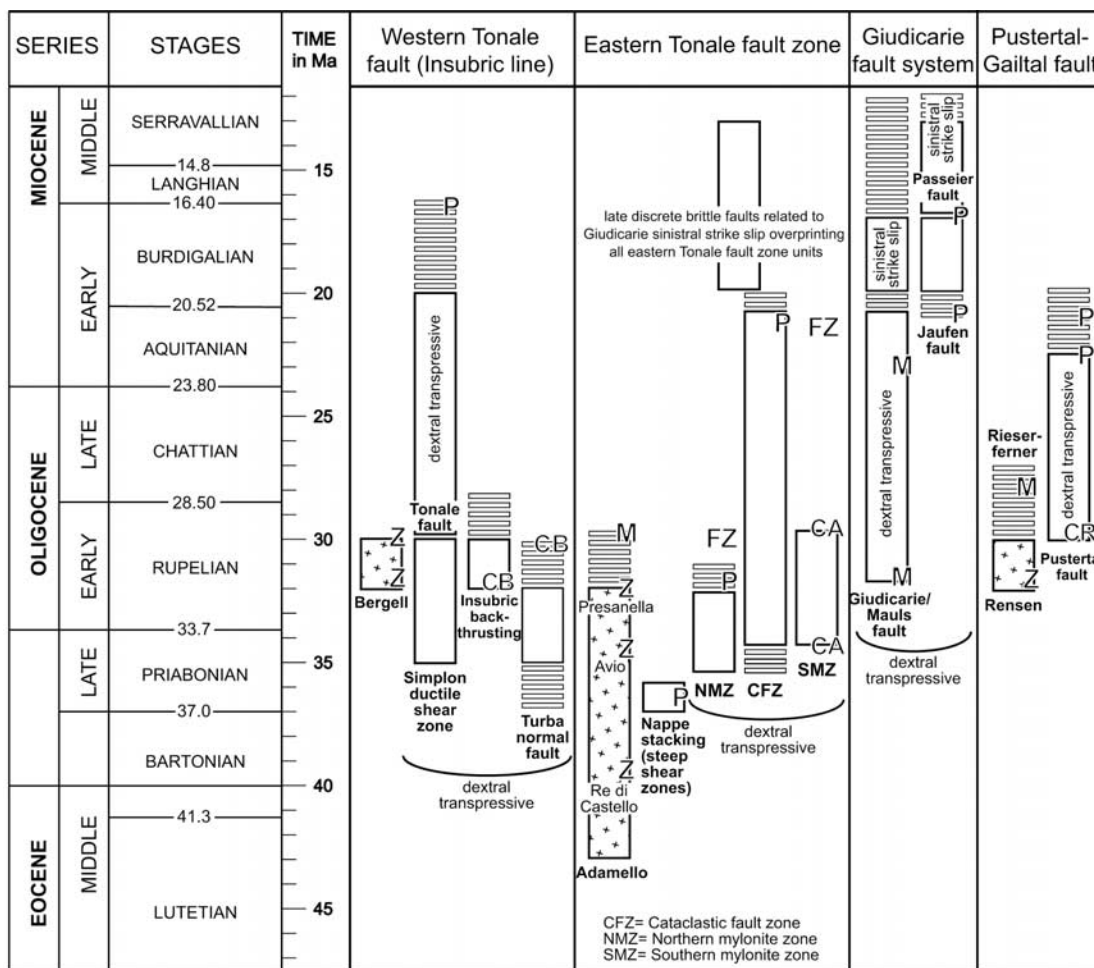
transition, i.e., at around 400°C in case of mylonites found in the north and between 250° and 280°C in case of the cataclasites in the south. Given a temperature difference of 120°–150°C, and a geothermal gradient of 26°–27°C/km, the vertical component of dextral strike-slip motion during the time interval from 35 to ~30 Ma and across the contact between Northern mylonite zone and Cataclastic fault zone is estimated to be 5 km.

[49] Mylonitization in the Southern mylonite zone and associated dextral strike-slip movements in this southern part of the Tonale fault zone started at ~34 Ma, i.e., contemporaneously with or slightly after the emplacement of the Avio intrusion. It must have stopped at ~29 Ma, because the Southern mylonite zone cooled below ~300°C by this time (Figure 13) when the thermal gradient vanished and the ambient temperatures fell below those required for viscous creep of quartz. Contact metamorphism of the Northern Adamello pluton may be described as “dynamic”, because it developed during contemporaneous strike-slip movements. After 29 Ma, ongoing dextral strike-slip activity concentrated within the Cataclastic fault zone. This stage occurred within a time period of extremely slow cooling after 30 Ma (Figure 13) and is characterized by exclusively cataclastic deformation. This brittle faulting, associated with pseudotachylyte formation, lasted until 20 Myr ago. This interpretation is compatible with a pseudotachylyte laser ablation Ar/Ar age of  $20.6 \pm 5.5$  Ma from the Cataclastic fault zone in Val Stavel [*Müller, 1998*]. Unfortunately, the total amount of dextral strike-slip motion accumulated between 35 and 20 Ma along the Tonale Fault Zone as a whole is difficult to assess, owing to the absence of marker horizons.

[50] Late discrete brittle faults, oriented approximately parallel to the Giudicarie strike slip, sinistrally offset all tectonic units of the eastern Tonale fault zone. This indicates that the Giudicarie Fault was active after 20 Myr ago, sinistrally offsetting the earlier formed Tonale-Pustertal fault zone, associated with dextral shearing.

### 8.4. Dynamic Contact Metamorphism

[51] Mapping across the Tonale fault zone, combined with microstructural evidence presented in section 6, clearly indicates that strike-slip movements along the Tonale fault zone caused a severely perturbed temperature-distance distribution adjacent to the northern Adamello pluton. Microstructural and textural records indicate that shear strain within the contact metamorphosed rocks increases towards the Tonale fault zone (from WSW to ENE, from the Avio to the Stavel section), and that strike-slip deformation is contemporaneous with the development of the contact aureole. Deformation partitioning and expansion of the shear zone towards the magmatic contact occurred slightly after temperature peak conditions. High temperature dynamic recrystallization microstructures were preserved, because retrogression during further cooling was localized into smaller zones. The geometry of the magmatic contact (e.g., bend of the northern pluton margin in Val Ogliolo, Figure 10) and the position of the Tonale fault zone determined by plate tectonic scale are probably responsible for strain partitioning between the contact metamorphosed Edolo schists and the



CA, CB and CR mean geologically constrained by contact relationships with Adamello, Bergell and Rieserferner/ Rensen pluton (intrusion ages), respectively  
 FZ= fission track analysis on zircon (Viola 2000, Viola et al. 2001, this study)  
 M= Rb/Sr and/or K/Ar analyses on different minerals (Borsi et al. 1979, Del Moro et al. 1983, Müller 1998, Müller et al. 2001)  
 P= Ar/Ar stepwise heating on pseudotachylyte (Müller 1998, Mancktelow et al. 2001, Müller et al. 2001)  
 Z= U/Pb single crystal analyses on zircons (Barth et al. 1989, Hansmann & Oberli 1991, von Blanckenburg et al. 1992, this study)

**Figure 14.** Timetable for four segments of the Periadriatic Fault System between Lago Maggiore in the west and the Tauern/Dolomites in the east. Local names of the faults are given; boxes indicate constrained activity of the fault; dashed boxes indicate activity as proposed from age determination or correlation. Age data from different studies have been compiled in this diagram; only the most reliable age data (with smallest error) indicating beginning or ending of activity have been included in the diagram. Chronostratigraphy is taken from *Berggren et al. [1995]* and *Hardenbol et al. [1998]*.

Southern mylonite zone and for the tendency of a more intense deformation away from the hottest, i.e., weakest part of the contact aureole.

[52] Strike-slip motion across the Tonale fault zone continuously brought cooler rocks (ambient temperature  $\approx 250^{\circ}\text{C}$ ) against the evolving aureole. Most likely this cooling effect is the cause of the observed telescoping of the isotherms, and of the unusually strong temperature depression in the outer part of the contact aureole. The restriction of contact metamorphic effects to the South-Alpine block is easily explained by advective cooling by the relatively cold Austro-Alpine basement during Tonale fault strike-slip movements.

[53] The localization of deformation within the Southern mylonite zone only occurred during advanced cooling of

contact metamorphism, and it also led to solid-state deformation along the magmatic contact. Hence the contact aureole of the Presanella and Avio intrusions differs from that of many other shallow plutons, where deformation is localized into very narrow shear zones and where static recrystallization microstructures predominate [e.g., *Buntebarth and Voll, 1991; Lind, 1996*].

### 8.5. Eastern Tonale Fault Zone in the Framework of the Periadriatic Fault System

[54] An age of 35 to 20 Ma (Figure 14) for the activity of the dextrally transpressive eastern Tonale fault zone is compatible with the age of dextral strike-slip movement derived for other branches of the Periadriatic Fault System,

situated west of our working area: (1) dextral shearing along the Simplon ductile shear zone between 35 and 30 Ma [Steck, 1990; Steck and Hunziker, 1994], contemporaneous with ascent and early stages of the emplacement of the Bergell pluton [Rosenberg et al., 1995; Berger et al., 1996], (2) backthrusting of the central Alps and related final emplacement of the Bergell pluton at 32–30 Ma [Schmid et al., 1989; Berger et al., 1996] along the western Tonale fault zone, and (3) subsequent purely dextral strike-slip movements along mylonites and cataclasites of the Tonale fault [Fumasoli, 1974; Schmid et al., 1989].

[55] The sinistral offset of all tectonic units of the eastern Tonale fault zone observed within the working area (Figure 3) indicates post-20 Ma sinistral offset of the Periadriatic Fault System by the Giudicarie fault (and related faults) [see Müller et al., 2001; Viola et al., 2001]. In conclusion, the last dextral strike-slip movements along the western parts of the Periadriatic Fault System took place during the Burdigalian (Figure 14). Note however, that dextral deformation continued further east until the mid-Miocene, related to sinistral movement along the Giudicarie fault, offsetting the Periadriatic Fault System, as is discussed below.

[56] In a larger scale Alpine context, the sinistral offset of the Periadriatic Fault system by the Giudicarie fault coincides with the onset of (1) thin-skinned folding and thrusting in the Lombardian Alps [Laubscher, 1990, 1996; Pieri and Groppi, 1981; Schönborn, 1992, 1999; Schmid et al., 1996], (2) the onset of exhumation of the Tauern window located in the footwall of the Brenner normal fault [Fügenshuh et al., 1997], and (3) lateral extrusion of the Eastern Alps [Ratschbacher et al., 1991; Frisch et al., 1998].

[57] Indirectly, the sinistral offset of the eastern Tonale fault zone has implications regarding the maximum possible amount of dextral offset on the Periadriatic Fault System. Schmid and Kissling [2000] postulated a total displacement of 100 km along Periadriatic Fault System and Simplon ductile shear zone, accommodating WNW directed indentation of the Adriatic block [Ceriani et al., 2001], while a series of other authors [e.g., Prosser, 1998; Müller et al., 2001; Viola et al., 2001] have interpreted relationships associated with the Giudicarie fault zone to greatly limit dextral displacements on the Periadriatic Fault System between 32 and 20 Ma. The latter authors interpreted the Giudicarie fault to represent a restraining bend of the Periadriatic Fault System, which reduces the maximum possible dextral offset along the E-W trending Periadriatic Fault System to a mere 30 km. We suggest, however, that the sinistral shears that overprint the eastern Tonale fault zone (Figure 3) are related temporally to sinistral displacements on the Giudicarie fault, and that all of these postdate dextral shearing within the Tonale fault zone. Note that the argument for activity on the Giudicarie fault being as old as 32 Ma comes from dating of fault rocks contained within it [Müller et al., 2001]. However, we argue that this age could reflect the preservation of older Tonale-Pustertal fault rocks that were captured within the intersecting younger Giudicarie fault

zone. This is analogous to the origin of tonalitic lamellae along the Giudicarie and Maults faults [e.g., Werling, 1992; Martin et al., 1993], interpreted as derived from a dextrally sheared tail of the Adamello pluton. Vertical displacements across the Periadriatic Fault System vary substantially along strike. The estimated total of 20 km found in locations south of the Lepontine dome [Schmid et al., 1989] decrease to the 5 km (before 30 Ma) derived for our working area. Subsequent vertical displacements along the eastern Tonale fault zone are not constrained by the available data. Further to the northeast close to the Maults fault (Figure 1) a vertical displacement of 4–5 km is observed since 24 Ma [e.g., Mancktelow et al., 2001].

[58] In summary, 35–20 Ma plutonism and dextral strike-slip faulting along the eastern Tonale fault zone (Figure 14) were coeval with backthrusting across the western Tonale fault zone [Schmid et al., 1989], orogen-parallel extension and early stages of lateral escape along Engadine and Tonale lines [e.g., Schmid and Froitzheim, 1993], and normal faulting across the Turba normal fault [Nievergelt et al., 1996; Liniger, 1992; Spillmann, 1993]. East of the working area, however, post-20 Ma sinistral strike-slip movements along the Giudicarie fault Zone did offset the former eastern extension of the Periadriatic Fault System, including the accompanying belt of Periadriatic intrusions [Rosenberg, 2004].

## 9. Conclusions

[59] This case study shows that pluton emplacement adjacent to a major active fault zone is associated with a complex interplay between contact metamorphism and shearing. Genetically, eastern Tonale fault zone and Adamello pluton are not connected to each other, but they mutually interact with each other due to spatial and temporal vicinity. Dextral shearing along the Tonale fault zone terminates pluton emplacement by ballooning towards the north and overprints previously solidified intrusions. The Adamello pluton and its thermal aureole cause expansion of the fault zone towards the pluton, i.e., southwards, thereby forming a Southern mylonite zone within the South-Alpine basement.

[60] Ongoing dextral shearing caused telescoping of the isotherms and advective cooling of the contact aureole within the Southern mylonite zone by the Austro-Alpine basement north of the Tonale fault zone. Initially cooling of pluton and country rocks was fast, but temperature remained constant at around 250°C thereafter, as indicated by combining U/Pb data on zircon for both Avio ( $34.6 \pm 1.0$  Ma) and Presanella intrusion ( $32.0 \pm 2.3$  Ma) with zircon fission track ages (22–20 Ma). The new age data not only constrain the evolution in time of the eastern Tonale fault zone and its different units at a local level. They also constrain the age of dextral transpression for the entire Periadriatic Fault System west of the Giudicarie line to have occurred within a time span from 35 to 20 Ma.

[61] The component of backthrusting motion decreased from some 20 km along the western continuation of the Tonale fault zone south of the Lepontine dome (central

Alps) to some 5 km in the study area. This scenario is associated with orogen-parallel extension east of the central Alps and early lateral escape of the Austro-Alpine units along the Tonale, Engadine and Turba fault zones. Previous estimates of the total amount of dextral strike-slip motion along the eastern Tonale fault zone to be in the order of 100 km remain poorly constrained. However, they must be of very limited extent after 20 Myr ago, when the Giudicarie line acted as a restraining bend. Younger dextral strike-slip displacements along the Periadriatic Fault System continued

east of our working area, as lateral extrusion of the Eastern Alps got underway at around 20 Myr ago.

[62] **Acknowledgments.** We thank E. Werling, P. Brack, S. Ceriani, S. Ellis, N. Froitzheim, R. Heilbronner, N. Mancktelow, C. Rosenberg, M. Tischler, and G. di Toro for fruitful discussions. Reviews by M. Brunel and A. Pfiffner significantly improved the paper. For technical support we thank Hans Rudi Rüegg and Willy Tschudin. This work was originally funded by the Swiss National Science Foundation, grants 20-49562.96 and 2000-055420.98. M. S. was supported by Swiss NF (research commission Basel 81BS-63210) and a Novartis stipendium while writing the manuscript.

## References

- Ahrendt, H. (1980), Die Bedeutung der Insubrischen Linie für den tektonische Bau der Alpen, *Neues Jahrb. Geol. Paläontol. Abh.*, 160, 336–362.
- Andreatta, C. (1935), La formazione gneissico-kinzigitica e le oliviniti di Val d' Ultimo (Alto Adige), *Mem. Mus. Storia Nat. Venezia Tridentina*, 3, 1–160.
- Andreatta, C. (1951), Carta geologica delle tre Venezie, Monte Cevedale F. 9, Uff. Idrogr. del Magistrato alle Acque di Venezia (LL, PP.), Venice, Italy.
- Andronicos, C. L., D. H. Chardon, L. S. Hollister, G. E. Gehrels, and G. J. Woodsworth (2003), Strain partitioning in an obliquely convergent orogen, plutonism, and synorogenic collapse: Coast Mountains Batholith, British Columbia, Canada, *Tectonics*, 22(2), 1012, doi:10.1029/2001TC001312.
- Barth, S., F. Oberli, and M. Meier (1989), U-Th-Pb systematics of morphologically characterized zircon and allanite: A high-resolution isotopic study of the Alpine Rensen pluton (northern Italy), *Earth Planet. Sci. Lett.*, 95, 235–254.
- Berger, A., C. Rosenberg, and S. M. Schmid (1996), Ascent, emplacement and exhumation of the Bergell pluton within the Southern Steep Belt of the central Alps, *Schweiz. Mineral. Petrogr. Mitt.*, 76, 357–382.
- Berggren, W. A., D. V. Kent, I. C. C. Swisher, and M. P. Aubry (1995), A revised Cenozoic geochronology and chronostratigraphy, in *Geochronology. Time Scales and Global Stratigraphic Correlation*, edited by W. A. Berggren et al., *Spec. Publ. SEPM Soc. Sediment. Geol.*, 54, 129–212.
- Bianchi, A., G. Dal Piaz, E. Callegari, and P. G. Jobstraibizer (1970), I tipi petrografici fondamentali del plutone dell'Adamello, *Mem. Ist. Geol. Min. Padova*, 27, 1–148.
- Bodorkos, S., P. A. Cawood, and N. H. S. Oliver (2000), Timing and duration of syn-magmatic deformation in the Mabel Downs Tonalite, northern Australia, *J. Struct. Geol.*, 22, 1181–1198.
- Bögel, H. (1975), Zur Literatur über die 'Periadriatische Naht,' *Verh. Geol. Bundesanst.*, 2–3, 163–199.
- Borsi, S., A. Del Moro, F. P. Sassi, and G. Zirpoli (1979), On the age of the Vedrette di Ries (Rieserferner) massif and its geodynamic significance, *Geol. Rundsch.*, 68, 41–60.
- Brack, P. (1983), Multiple intrusions—Examples from the Adamello batholith (Italy) and their significance on the mechanisms of intrusion, *Mem. Soc. Geol. Ital.*, 26, 145–157.
- Brown, M., and G. S. Solar (1999), The mechanism of ascent and emplacement of granite magma during transpression: A syntectonic granite paradigm, *Tectonophysics*, 312, 1–33.
- Buntebarth, G., and G. Voll (1991), Quartz grain coarsening by collective crystallization in contact quartzites, in *Equilibrium and Kinetics in Contact Metamorphism*, edited by G. Voll et al., pp. 251–265, Springer-Verlag, New York.
- Callegari, E., and G. Dal Piaz (1973), Field relationship between the main igneous masses of the Adamello intrusive massif (Northern Italy), *Mem. Ist. Geol. Min. Padova*, 29, 1–39.
- Ceriani, S., B. Fügenschuh, and S. M. Schmid (2001), Multi-stage thrusting at the "Penninic Front" in the Western Alps between Mont Blanc and Pelvoux massifs, *Int. J. Earth Sci.*, 90, 685–702.
- Cornelius, H. P., and M. Furlani-Cornelius (1928), Bericht über geologische Untersuchungen an der insubrischen Linie zwischen Tessin und Tonalepaß, in *Akademischer Anzeiger*, vol. 4, 3 pp., Akad. der Wiss., Vienna.
- Cornelius, H. P., and M. Furlani-Cornelius (1930), Die Insubrische Linie vom Tessin bis zum Tonalepaß, *Denkschr. Akad. Wiss., Math.-Naturwiss. Kl.*, 102, 207–301.
- Davidson, C., L. S. Hollister, and S. M. Schmid (1992), Role of melt in the formation of a deep-crustal compressive shear zone: The MacLaren glacier metamorphic belt, south central Alaska, *Tectonics*, 11, 348–359.
- Del Moro, A., G. Pardini, C. Quercioli, I. M. Villa, and E. Callegari (1983), Rb/Sr and K/Ar chronology of Adamello granitoids, Southern Alps, *Mem. Soc. Geol. Ital.*, 26, 285–299.
- Fisch, H. (1989), Zur Kinematik der südlichen Steilzone der Zentralalpen, E von Bellinzona, *Schweiz. Mineral. Petrogr. Mitt.*, 69, 377–392.
- Frey, M., J. Desmons, and F. Neubauer (1999), Map of alpine metamorphism, in *Metamorphic Maps of the Alps*, *Schweiz. Mineral. Petrogr. Mitt.*, 79(1), enclosure.
- Frisch, W., J. Kuhlemann, I. Dunkl, and A. Brugel (1998), Palinspastic reconstruction and topographic evolution of the eastern Alps during late Tertiary tectonic extrusion, *Tectonophysics*, 297, 1–15.
- Fügenschuh, B., and S. M. Schmid (2003), Late stages of deformation and exhumation of an orogen constrained by fission-track data: A case study in the Western Alps, *Geol. Soc. Am. Bull.*, 115, 1425–1440.
- Fügenschuh, B., D. Seward, and N. Mancktelow (1997), Exhumation in a convergent orogen: The western Tauern Window, *Terra Nova*, 9, 213–217.
- Fumasoli, M. (1974), Geologie des Gebietes nördlich und südlich der Jorio-Tonale-Linie im Westen von Gravedona, *Mitt. Geol. Inst. Eidg. Tech. Hochsch. Univ. Zürich*, 194, 1–230.
- Galbraith, R. F. (1981), On statistical models for fission-track counts, *Math. Geol.*, 13, 471–478.
- Galbraith, R. F., and G. M. Laslett (1993), Statistical models for mixed fission track ages, *Nucl. Tracks Radiat. Meas.*, 21, 459–470.
- Gansser, A. (1968), The Insubric Line, a major geotectonic problem, *Schweiz. Mineral. Petrogr. Mitt.*, 48, 123–143.
- Hammer, W., and G. B. Trener (1908), Erläuterungen zur geologischen Karte der Österr.-Ungar. Monarchie: Bormio und Passo del Tonale, *K. K. Geol. Reichsanst.*, 54 pp.
- Hansmann, W., and F. Oberli (1991), Zircon inheritance in an igneous rock suite from the southern Adamello batholith (Italian Alps): Implications for petrogenesis, *Contrib. Mineral. Petrol.*, 107, 501–518.
- Hardenbol, J., J. Thierry, M. B. Farley, T. Jacquin, P.-C. De Graciansky, and P. R. Vail (1998), Mesozoic and Cenozoic sequence chronostratigraphic framework of European basins, in *Mesozoic and Cenozoic Sequence Stratigraphy of European Basins*, edited by P.-C. De Graciansky et al., *Spec. Publ. SEPM Soc. Sediment. Geol.*, 60, 3–13.
- Heitzmann, P. (1987), Evidence of late Oligocene/early Miocene backthrusting in the central Alpine "root zone," *Geodyn. Acta*, 1, 183–192.
- Hunziker, J. C., J. Desmons, and A. J. Hurford (1992), Thirty-two years of geochronological work in the central and Western Alps: A review on seven maps, *Mem. Geol. Lausanne*, 13, 59 pp.
- John, B. E., and J. D. Blundy (1993), Thermal and mechanical aspects of granitoid emplacement in the southern Adamello Massif, Italy, *Geol. Soc. Am. Bull.*, 105, 2108–2120.
- John, B. E., and H. Stünitz (1997), Evidence for magmatic fracturing and small-scale melt segregation during pluton emplacement, in *Processes of Melt Segregation*, edited by J.-L. Bouchez and J. Clemens, pp. 55–74, Kluwer Acad., Norwell, Mass.
- Lardelli, T. (1981), Die Tonalelinie im unteren Veltlin, Julius Druck und Verlag, Zürich.
- Laubscher, H. P. (1983), The late alpine (Periadriatic) intrusions and the Insubric Line, *Mem. Soc. Geol. Ital.*, 26, 21–30.
- Laubscher, H. P. (1990), The problem of the deep structure of the Southern Alps: 3-D material balance considerations and regional consequences, *Tectonophysics*, 176, 103–121.
- Laubscher, H. (1996), Shallow and deep rotations in the Miocene Alps, *Tectonics*, 15, 1022–1035.
- Lind, A. (1996), Microstructural stability and the kinetics of textural evolution, Ph.D. thesis, Univ. of Leeds, UK.
- Liniger, M. (1992), Der Ostalpin-Penninische Grenzbereich im Gebiet der nördlichen Margna-Decke (Graubünden, Schweiz), Ph.D. thesis, Eidg. Tech. Hochsch. (ETH), Zürich.
- Lippitsch, R., E. Kissling, and J. Ansorge (2003), Upper mantle structure beneath the Alpine orogen from high-resolution teleseismic tomography, *J. Geophys. Res.*, 108(B8), 2376, doi:10.1029/2002JB002016.
- Malaroda, R. (1952), Nuovi lembi di terreni permotriassici lungo la Linea del Tonale nell'alta val di Sole, *Atti Ist. Veneto Sci. Lett. Arti, Cl. Sci. Mat. Nat.*, 110, 141–151.
- Mancktelow, N. S., D. F. Stöckli, B. Grollimund, W. Müller, B. Fügenschuh, G. Viola, D. Seward, and I. M. Villa (2001), The DAV and Periadriatic fault systems in the Eastern Alps south of the Tauern window, *Int. J. Earth Sci.*, 90, 593–622.
- Martin, S., G. Prosser, and L. Santini (1991), Alpine deformation along the Periadriatic lineament in the Italian Eastern Alps, *Ann. Tectonicae*, 5, 118–140.
- Martin, S., G. Prosser, and L. Morten (1993), Tectonomagmatic evolution of sheeted plutonic bodies along the north Giudicarie line (northern Italy), *Geol. Rundsch.*, 82, 51–66.
- Mendum, J. R. (1976), The structure and metamorphic geology of the Tonale Pass Area, northern Italy, Ph.D. thesis, Univ. of Edinburgh, UK.

- Moyen, J. F., A. Nedelec, H. Martin, and M. Jayananda (2003), Syntectonic granite emplacement at different structural levels: The Closepet granite, South India, *J. Struct. Geol.*, 25, 611–631.
- Müller, W. (1998), Isotopic dating of deformation using microsampling techniques: The Evolution of the Periadriatic Fault System (Alps), Ph.D. thesis, Eidg. Tech. Hochsch. (ETH), Zürich.
- Müller, W., G. Prosser, N. S. Mancktelow, I. M. Villa, S. P. Kelley, G. Viola, and F. Oberli (2001), Geochronological constraints on the evolution of the Periadriatic Fault System (Alps), *Int. J. Earth Sci.*, 90, 623–653.
- Nievergelt, P., M. Liniger, N. Froitzheim, and R. F. Mählmann (1996), Early to mid Tertiary crustal extension in the Central Alps: The Turba Mylonite Zone (Eastern Switzerland), *Tectonics*, 15, 329–340.
- Panozzo Heilbronner, R., and C. Pauli (1993), Integrated spatial and orientation analysis of quartz [c]-axes by computer-aided microscopy, *J. Struct. Geol.*, 15, 369–382.
- Pattison, D. R. M., and B. Harte (1991), Petrography and mineral chemistry of pelites, in *Equilibrium and Kinetics in Contact Metamorphism*, edited by G. Voll et al., pp. 135–179, Springer-Verlag, New York.
- Peacock, S. M. (1989), Thermal modeling of metamorphic pressure-temperature-time paths: A forward approach, in *Metamorphic Pressure-Temperature-Time Paths, Short Course Geol. Ser.*, vol. 7, edited by F. S. Spear and S. M. Peacock, pp. 57–102, AGU, Washington, D. C.
- Pfiffner, O. A., and J. G. Ramsay (1982), Constraints on geological strain rates: Arguments from finite-strain states of naturally deformed rocks, *J. Geophys. Res.*, 87, 311–321.
- Pieri, M., and G. Groppi (1981), Subsurface geological structure of the Po plain, Italy, in *Progetto Finalizzato Geodinamica, CNR Publ. 414*, pp. 113–119, Cons. Naz. delle Ric., Rome, Italy.
- Prosser, G. (1998), Strike-slip movements and thrusting along a transpressive fault zone: The North Giudicarie line (Insubric line, northern Italy), *Tectonics*, 17, 921–937.
- Ramsay, J. G. (1989), Emplacement kinematics of a granite diapir: The Chindamora batholith, Zimbabwe, *J. Struct. Geol.*, 11, 191–209.
- Ratschbacher, L., W. Frisch, H.-G. Linzer, and O. Merle (1991), Lateral extrusion in the Eastern Alps: 2. Structural analysis, *Tectonics*, 10, 257–271.
- Rosenberg, C. L. (2004), Shear zones and magma ascent: A model based on a review of the Tertiary magmatism in the Alps, *Tectonics*, 23, TC3002, doi:10.1029/2003TC001526.
- Rosenberg, C. L., A. Berger, and S. M. Schmid (1995), Observations from the floor of a granitoid pluton: Inferences on the driving force of final emplacement, *Geology*, 23, 443–446.
- Salomon, W. (1905), Die alpine-dinarische Grenze, *Verh. K. K. Geol. Reichsanst.*, 341–343.
- Schmid, S. M., and N. Froitzheim (1993), Oblique slip and block rotation along the Engadine line, *Eclogae Geol. Helv.*, 86, 569–593.
- Schmid, S. M., and E. Kissling (2000), The arc of the Western Alps in the light of geophysical data on deep crustal structure, *Tectonics*, 19, 62–85.
- Schmid, S. M., A. Zingg, and M. Handy (1987), The kinematics of movements along the Insubric Line and the emplacement of the Ivrea Zone, *Tectonophysics*, 135, 47–66.
- Schmid, S., H. R. Aebli, F. Heller, and A. Zingg (1989), The role of the Periadriatic Line in the tectonic evolution of the Alps, in *Alpine Tectonics*, edited by M. P. Coward, D. Dietrich, and R. G. Park, *Geol. Soc. Spec. Publ.*, 45, 153–171.
- Schmid, S. M., O. A. Pfiffner, N. Froitzheim, G. Schönborn, and E. Kissling (1996), Geophysical-geological transect and tectonic evolution of the Swiss-Italian Alps, *Tectonics*, 15, 1036–1064.
- Schmid, S. M., B. Fügenschuh, and R. Lippitsch (2003), The Western Alps-Eastern Alps transition: Tectonics and deep structure, *Mem. Sci. Geol.*, 54, 257–260.
- Schönborn, G. (1992), Alpine tectonics and kinematic models of the central Southern Alps, *Mem. Sci. Geol.*, 44, 229–393.
- Schönborn, G. (1999), Balancing cross sections with kinematic constraints: The Dolomites (northern Italy), *Tectonics*, 18, 527–545.
- Seward, D. (1989), Cenozoic basin histories determined by fission track dating of basement granites, South Island, New Zealand, *Chem. Geol.*, 122, 249–258.
- Spalla, M. I., E. Carminati, S. Ceriani, A. Olivia, and D. Battaglia (1999), Influence of deformation partitioning and metamorphic re-equilibration on P-T path reconstruction in the pre-Alpine basement of central Southern Alps (northern Italy), *J. Metamorph. Geol.*, 17, 319–336.
- Spillmann, P. (1993), Die Geologie des penninisch-ostalpinen Grenzbereichs im südlichen Berninagebirge, Ph.D. thesis, Eidg. Tech. Hochsch. (ETH), Zürich.
- Steck, A. (1990), Une carte des zones de cisaillement ductile des Alpes Centrales, *Eclogae Geol. Helv.*, 83, 603–626.
- Steck, A., and J. Hunziker (1994), The Tertiary structural and thermal evolution of the Central Alps—Compressional and extensional structures in an orogenic belt, *Tectonophysics*, 238, 229–254.
- Steenken, A., S. Siegesmund, and T. Heinrichs (2000), The emplacement of the Rieserferner Pluton (Eastern Alps, Tyrol): Constraints from field observations, magnetic fabrics and microstructures, *J. Struct. Geol.*, 22, 1855–1873.
- Stipp, M. K. D. (2001), Dynamic recrystallization of quartz in fault rocks from the eastern Tonale line (Italian Alps), Ph.D. thesis, Univ. Basel, Switzerland.
- Stipp, M., and S. Schmid (1998), Evidence for the contemporaneity of movements along the Tonale line and the intrusion of parts of the Adamello batholith, *Mem. Sci. Geol.*, 50, 89–90.
- Stipp, M., H. Stünitz, R. Heilbronner, and S. M. Schmid (2002a), The eastern Tonale fault zone: A “natural laboratory” for crystal plastic deformation of quartz over a temperature range from 250°C to 700°C, *J. Struct. Geol.*, 24, 1861–1884.
- Stipp, M., H. Stünitz, R. Heilbronner, and S. M. Schmid (2002b), Dynamic recrystallization of quartz: Correlation between natural and experimental conditions, in *Deformation Mechanisms, Rheology and Tectonics: Current Status and Future Perspectives*, edited by S. De Meer et al., *Geol. Soc. Spec. Publ.*, 200, 171–190.
- Trener, G. B. (1906), Geologische Aufnahme im nördlichen Abhang der Presanellagruppe, *Jahrb. K. K. Geol. Reichsanst.*, 56, 405–496.
- Vernon, R. H. (1999), Quartz and feldspar microstructures in metamorphic rocks, *Can. Mineral.*, 37, 513–524.
- Viola, G. (2000), Kinematics and timing of the Periadriatic fault system in the Giudicarie region (central-eastern Alps), Ph.D. thesis, Eidg. Tech. Hochsch. (ETH), Zürich.
- Viola, G., N. S. Mancktelow, and D. Seward (2001), Late Oligocene-Neogene evolution of Europe-Adria collision: New structural and geochronological evidence from the Giudicarie fault system (Italian Eastern Alps), *Tectonics*, 20, 999–1020.
- Vogler, W. S., and G. Voll (1981), Deformation and metamorphism at the south-margin of the Alps, east of Bellinzona, Switzerland, *Geol. Rundsch.*, 70, 1232–1262.
- von Blanckenburg, F., G. Früh-Green, K. Diethelm, and P. Stille (1992), Nd-, Sr-, O-isotopic and chemical evidence for a two stage contamination history of mantle magma in the Central-Alpine Bergell intrusion, *Contrib. Mineral. Petrol.*, 110, 33–45.
- von Blanckenburg, F., H. Kagami, A. Deutsch, F. Oberli, M. Meier, M. Wiedenbeck, S. Barth, and H. Fischer (1998), The origin of Alpine plutons along the Periadriatic Lineament, *Schweiz. Mineral. Petrogr. Mitt.*, 78, 55–66.
- von Gosen, W. (1989), Fabric developments and the evolution of the Periadriatic Lineament in southeast Austria, *Geol. Mag.*, 126, 55–71.
- Werling, E. (1992), Tonale-, Pejo- und Giudicarie-Linie: Kinematik, Mikrostrukturen und Metamorphose von Tektoniten aus räumlich interferierenden aber verschiedenartigen Verwerfungszonen, Ph.D. thesis, Eidg. Tech. Hochsch. (ETH), Zürich.
- Wiedenbeck, M. (1986), Structural and isotopic age profile across the Insubric Line, Mello, Valtellina, N. Italy, *Schweiz. Mineral. Petrogr. Mitt.*, 66, 211–227.
- Zarske, G. (1989), Gefügekundliche und kristallogeo-logische Untersuchungen zur alpinen Störungskinetik im Umbiegunsbereich von Tonale- und Giudicarie-Linie, *Gött. Arb. Geol. Paläontol.*, 38, 142 pp.

B. Fügenschuh, S. M. Schmid, and H. Stünitz, Department of Earth Sciences, Basel University, Bernoullistrasse 32, CH-4056 Basel, Switzerland.

L. P. Gromet, Department of Geological Sciences, Brown University, P.O. Box 1846, Providence, RI 02912, USA.

M. Stipp, Geological Institute, Albert-Ludwigs-University, Albertstrasse 23b, D-79104 Freiburg, Germany. (michael.stipp@geologie.uni-freiburg.de)